

VĚDECKÉ SPISY VYSOKÉHO UČENÍ TECHNICKÉHO V BRNĚ

Edice Habilitační a inaugurační spisy, sv. 735

ISSN 1213-418X

Jan Čechal

**SELF-ASSEMBLY
ON SOLID SURFACES:
A STUDENT'S GUIDE**

VYSOKÉ UČENÍ TECHNICKÉ V BRNĚ
CEITEC

doc. Ing. Jan Čechal, Ph.D.

**SELF-ASSEMBLY ON SOLID SURFACES:
A STUDENT'S GUIDE**

RUKOVĚŤ STUDENTOVA
K SAMOUSPOŘÁDÁVÁNÍ NA POVRŠÍCH

THESIS OF THE INAUGURATION LECTURE
IN APPLIED PHYSICS



BRNO 2022

KEYWORDS

Surfaces; Self-Assembly; Nanostructures; Molecules; Organic Semiconductors; Metal-Organic Networks; Graphene; Phase Transitions; Kinetics; Deprotonation; Tilings; Electron Beam; Low-Energy Electron Microscopy, LEEM; Scanning Tunneling Microscopy, STM; X-ray Photoelectron Spectroscopy, XPS.

KLÍČOVÁ SLOVA

Povrchy; Samouspořádávání; Nanostruktury; Molekuly; Organické polovodiče; Grafen; Metaloorganické sítě; Fázové přechody; Kinetika; Deprotonace; Teselace; Elektronový svazek; Rastrovací tunelová mikroskopie, STM; Nízkoenergieová elektronová mikroskopie, LEEM; Rentgenová fotoelektronová spektroskopie, XPS.

This thesis was reviewed by

Matthias Blatnik, Zdeněk Jakub, Radek Kalousek, Tomáš Krajňák, Anna Kurowská, Anton Makoveev, Jakub Planer, Pavel Pocházka, Azin Shahsavar, Jiří Spousta, and Vojtěch Uhlíř.

© Jan Čechal, 2022

ISBN 978-80-214-6098-0

ISSN 1213-418X

Contents

1	Introduction	1
2	Goals of Nanotechnology	2
3	Molecular Self-Assembly	4
4	Low-Energy Electron Microscopy	6
5	Scanning Tunneling Microscopy and X-ray Photoelectron Spectroscopy	8
6	Thermal Deprotonation	10
7	Role of the Substrate	12
8	Transformation Kinetics	14
9	No unit cell of the α phase	16
10	Tilings	18
11	Electron-Beam Induced Transformations	20
12	Vision: Organic Electronics	22
13	Vision: Metal-Organic Networks on 2D Materials	24
14	Research Group: Molecular Nanostructures at Surfaces	26
	References	28
	Rights and Permissions	34
	Abstract/Abstrakt	35

Author



Jan Čechal was born on February the 20th, 1978, in Kyjov. His first contact with science and education was at the astronomical observatory in Ždánice, where he participated in a program on the visual observation of variable stars and gave lectures and guided observations with telescopes for school excursions and the general public.

However, the lack of experiments in astronomy led him to a different part of physics. He graduated in “Physical Engineering” at the Brno University of Technology (BUT) in 2001. During his Ph.D., Jan Čechal explored the possibilities of morphological analysis by X-ray photoelectron spectroscopy and employed synchrotron radiation for analysis of surface structures under the supervision of Prof. Petr Dub.

After his Ph.D., he continued his research at the Institute of Physical Engineering (group of Prof. Šikola) at BUT on hybrid top-down/bottom-up lithographic approaches for preparing nanostructures. To get more interdisciplinary background and to pursue his interest in surface-confined molecular systems, he joined the group of Prof. Klaus Kern at Max-Planck Institute for Solid State Research in Stuttgart (Germany) under an individual Marie Curie fellowship in 2010.

In 2012, after returning to Brno, he participated in developing the newly established research center CEITEC in Brno. Besides his research within the “Fabrication and Characterisation of Nanostructures” research group, he significantly contributed to establishing the CF Nano UHV laboratory and the definition of its research lines. He participated in the preparation of several large-scale development projects (Teaming and Twinning actions, large national projects).

Jan Čechal became Research Group Leader at CEITEC in 2018, focusing the research on the self-assembly of molecular nanostructures on surfaces, developing a quantitative description of its kinetics, and revealing the possibilities to steer these processes by active graphene substrates as described in this thesis. At the time of writing this thesis, he leads a group comprising 5 postdoctoral researchers, 5 Ph.D., and 6 undergraduate students.

Since his Ph.D. studies, Jan Čechal has been teaching at the Faculty of Mechanical Engineering both students of general engineering programs (physics) and “Physical Engineering and Nanotechnology” specialization. The specialized courses include “Surfaces and Thin Films”, “Theoretical and Continuum Mechanics”, “Diploma Seminar”, and lectures within “Microscopy and Spectroscopy” and “Diagnostic of Nanostructures” courses. So far, he supervised 1 Ph.D., 14 master’s, and 14 bachelor’s students who successfully defended their final theses.

Jan Čechal co-authored over 50 peer-reviewed papers that received more than 600 citations (h-index 14).

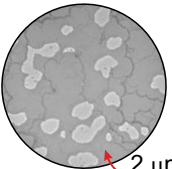
1 Introduction

Dear reader, you are holding the thesis of my inauguration lecture. A thesis of a lecture has loose formal requirements on its content and style, so I can follow an unusual path to create something I have never done so far. I intended to prepare a guide for students coming to our laboratory. This text should provide them with the necessary background: a collection of sections will guide them through the field we are working in and, more importantly, many open questions they can ask their colleagues or search for on the web to extend their knowledge. Each double page is dedicated to one topic, and the text is complemented with graphical boxes (see box 2) to highlight important concepts and our results. Will this graphical concept work? I am not sure, but, as an experimentalist, I will try!

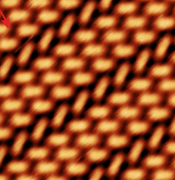
In our laboratory, we do *surface science* research on molecular nanostructures on solid surfaces. We apply a complex, multimethod approach (see box 1) to study *molecular self-assembly*, which enables fabricating nanostructures with atomic precision at large scales. This thesis will guide you into this topic. The general concepts are followed by sketching the research we perform in our laboratory. The thesis finishes with our visions, i.e., directions where we are heading at the moment (of course, these sections will get outdated as time passes by). However, this thesis will not provide complete knowledge; you are expected to go deeper yourself. I hope that your discoveries will go far beyond this thesis. Enjoy the journey to the world of self-assembly.

FEATURE 1

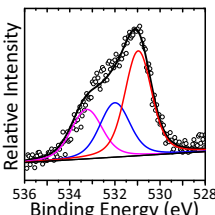
Surfaces: a complex approach
In our laboratory, we employ a set of complementary methods to get a complete picture of molecular phases and their transformations.



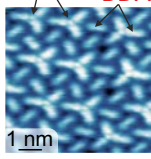
LEEM:
mesoscale morphology and structure



STM:
structure at atomic and molecular level.



XPS:
bond-specific chemical analysis.



OUR RESULTS
Our results are shown in light blue frames.

All these methods are detailed in the following sections.

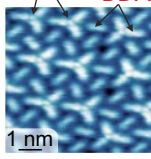
HOW TO READ THIS THESIS 2

CONVERSATION

What are conversations?
These dialogues pinpoint interesting features in a space-efficient way.

OUR RESULTS

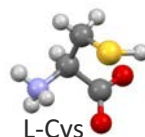
Our results are shown in light blue frames.



Ag atoms
BDA
1 nm


FEATURE

Feature boxes.
Feature boxes summarize key knowledge from literature and textbooks. The source is referenced as follows:




L-Cys

Key reference: [www](#)
F. Wu et al.,
Nano Lett. **22**
(2022), 2915.



KEY PUBLICATION

In this box, we provide the key reference to our work for given double-page dedicated to a particular topic.



1

2 Goals of Nanotechnology

For decades, miniaturization was driven by the needs of the electronic industry as dictated by Moore's law: the number of transistors in a dense integrated circuit (e.g., processor) doubles every two years. Along with this trend, the size of a transistor, and the end-user price will decrease while the computing power increases. "Faster, smaller, cheaper" was the mantra of the electronic industry. However, as the technology of fabricating small "things" and our capabilities to analyze their properties advanced, it has become evident that materials with a small size display fascinating properties distinct from that of bulk material. In this view, the field of nanotechnology quickly grew (see box 3), promising to provide new materials and functionalities.

There are three main directions in nanotechnology (see boxes 4–6). In the first one, we aim to reduce the size of the objects while keeping their functionality as in the already mentioned integrated circuits. Smaller structures produce less heat, enable faster operation, and consume less material for their manufacturing. In the same way, downsizing the elements in magnetic storage media would offer a higher density of stored information and faster read-out; however, the stability of magnetization becomes problematic below a certain size.¹

The second direction pursues the new physical properties related to reduced size or dimensionality. Electrons spatially confined in nanoparticles behave as in artificial atoms. Hence, by changing the nanoparticle size, the position of electron energy levels can be tuned, which is utilized, e.g., in electroluminescent quantum dots that emit light of specific colors.² Confined electrons inside a metal nanoobject can resonantly oscillate when interacting with light waves, which leads to size-dependent light absorption and a huge enhancement of electric fields in the vicinity of the irradiated nanoobjects below the diffraction limit.³ In materials with reduced dimensionality, e.g., graphene and 2D materials or their heterointerfaces, new physical phenomena appear; they are related to, e.g., energy-band structure, quantum confinement effects, or proximity to materials in their surroundings.⁴

The third direction harnesses properties of surfaces and interfaces that are different from the bulk due to the broken translation symmetry in one direction and missing bonds to former bonding partners. When downsizing the objects, surface properties become more pronounced, and for nanometer-sized objects, their properties can become dominant over the bulk ones. One of the most important surface properties is the catalytic activity, which originates only in specific active sites on the surface.⁵ For the functionality of catalysts, the bulk is often not relevant. Therefore, reducing the size of catalytic particles saves the expensive material while enhancing the relative amount of active sites. Surfaces are also important starting points for

FEATURE 3

New prospects for nanotechnology.
Editorial to inauguration issue on Nature Nanotechnology defining the challenges in the field.

EDITORIAL

nature nanotechnology Vol. 1 No. 1 October 2006

WWW 

Small is different

Nanoscience and nanotechnology offer fundamental challenges in research and the possibility of a new industrial revolution. This presents opportunities for all sorts of scientists and engineers.

Editorial to ACS Nano on nanotechnology targets beyond miniaturization.

Different and More Powerful, Not Just Smaller, Faster, Cheaper EDITORIAL

A major driving force behind the development of new tools and techniques in nanoscience has been the ability to produce electronic devices and circuits with smaller dimensions, faster processing times, and cheaper production costs. "Faster, smaller, cheaper" has become a mantra for the semiconductor industry and has motivated further development of established nanofabrication tools and methods, new capabilities are being enabled by chemical methods of nanofabrication and the resulting creation of nanoscale chemical patterns.¹ Likewise, a plethora of clever alternative methods for pat-

WWW 

FEATURE 4

Bulk properties.
Physical properties that are defined by the bulk, e.g., magnetic ordering, require a certain number of atoms to remain stable at room temperature. Hence, downsizing the magnets starts to face size limits. Prominently, the downsizing was the primary focus of the electronic industry following Moore's law.

IBM 2-nm GAA-FET Technology



Source: IBM

2 nm devices imaged by TEM.

www 

FEATURE 5

Quantum size effects.
Below a certain size, quantum effects, e.g., confinement, become apparent. Quantum dots (QDs) behave as artificial atoms, but their energy levels can be tuned by their size. QDs then emit light of a color given by their size.



1.0 1.5 2.0 2.5 3.0
QD size in nm

Samsung QLED Technology

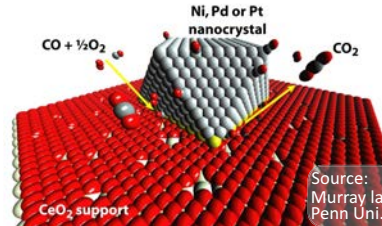


ZnTeSe/ZnSe/ZnS core/shell/shell quantum dots.


www 

FEATURE 6

Surface properties.
Surfaces and interfaces display properties different from the bulk. Undercoordinated atoms present on surfaces, especially in kink positions, are often reactive and form active centers of heterogeneous catalysts. The recent trend is to reduce the size of catalytic particles to the single atom limit.



Source: Murray lab Penn Uni.

www 

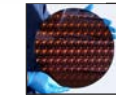
the growth of materials, e.g., above mentioned integrated circuits. Surfaces provide templates for the growth of functional 1D or 2D nanostructures via bottom-up fabrication, e.g., via molecular self-assembly, which is described in the next section.

There are two distinct approaches for fabrication of nanostructures: top-down and bottom-up (see box 7).¹ In the top-down one, we shape the larger objects into small nanostructures, e.g., metallic layer into nanosized plasmonic antennas. In recent years there was enormous progress in lithography to enable downscaling the electronic circuit components. Simultaneously, alternative fabrication methods were developed, like focused ion beam milling or deposition. The bottom-up approach becomes advantageous as the size of required objects come close to a few atoms. In this approach, we build more complex nanostructures from elementary building blocks, e.g., atoms and molecules. In this way, we can reach atomic precision in controlling and shaping the matter in required structures.


The development of fabrication methods goes hand in hand with our capabilities to analyze the properties of fabricated nanostructures. The traditional methods of taking information from a large area/volume are being adapted to measure single nanoobjects, like tip-enhanced Raman and infrared spectroscopy or microscopic capabilities added to XPS. Nowadays, electron microscopes offer additional spectroscopic modes beyond imaging, e.g., electron energy loss spectroscopy in TEM or Auger electron spectroscopy or cathodoluminescence spectroscopy SEM. In this thesis, we will, however, employ more traditional surface-science techniques that have also become indispensable in nanostructure analysis.

FEATURE 7

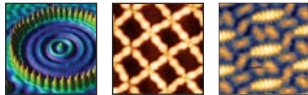
Top down and bottom up approaches.
Fabrication of nanostructures can follow two approaches: either we shape existing objects into desired structures or assemble them from basic building blocks. The first one, lithography, forms the basis of manufacturing in the electronic industry. The second one holds the promise of an atomically precise fabrication.




Top down



Cappadocia, Turkey.




Bottom up



James May's Lego House.

← →

www 

3 Molecular Self-Assembly

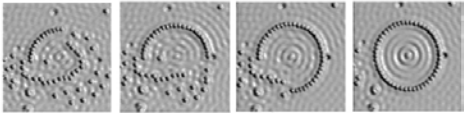
Nanostructures can be fabricated with ultimate precision by positioning individual atoms by the STM tip (see box 8). However, such a serial process would hardly ever become a viable technology. To realize that, let us change the scale by 10^7 , i.e., 1 nm to 1 cm. In this scale, the area equivalent to a 4-inch wafer is the same as ten times the area of the Czech Republic. Production on this scale would be a tedious job, and we should develop other strategies for atomically precise manufacturing. One prospective candidate is molecular self-assembly (see box 9).⁶ Instead of atoms, we use molecules as elementary building blocks with predefined properties. Molecules bring the advantage of high chemical tunability by employing mainly the abundant elements like carbon, oxygen, nitrogen, and sulfur combined with only a tiny fraction of atoms of rare materials.

The ordering of adsorbed molecules at solid surfaces is governed by the interplay between intermolecular and molecule-substrate interactions. Key principles of self-assembly of long-range ordered molecular structures are effective correction of defective binding motifs and self-selection of bonding partners.⁷ The error correction is the ability to eliminate transiently formed defective structures, i.e., to break the bonds that do not present an ideal structure with the lowest energy and replace them with the “correct ones”. Self-selection and self-recognition enable the selection of a particular component from multicomponent mixtures and its attachment to the desired position; they are possible thanks to the dynamic error correction process.

For efficient error correction, the bonding should be reversible at temperatures at which the employed molecules remain stable. This precludes strong covalent bonds, and, therefore, weaker intermolecular interactions should be used instead. These cover hydrogen and halogen bonds between suitable functional groups, coordination bonds between metal atoms and ligands, or substrate-mediated interactions that do not have a counterpart in bulk or solution (see Section 7). Another condition of efficient error correction is free diffusion of the molecules over the substrate, which ensures that “correct” binding partners reach a particular site.


FEATURE 8

Building structures atom-by-atom.
By the STM tip, it is possible to push, pull, or transport individual atoms over the surface. In this way, artificial nanostructures can be formed with atomic precision.



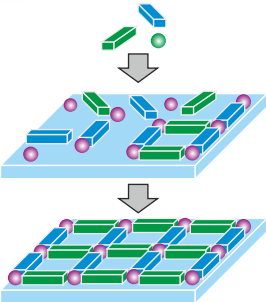
Forming
a quantum coral from Fe atoms.

Key reference:
M. F. Crommie,
Science **262**
(1993), 218.

WWW



FEATURE 9


Molecular self-assembly at surfaces.
Employing reversible interactions enables the growth of nanostructures in a dynamic equilibrium with their surroundings. Reversible interactions enable the correction of transient defective motifs, resulting in highly ordered structures. Self-selection of components ensures that only correct bonding motifs are formed in the mixture of elemental building blocks provided to the surface.



A video presenting self-assembly at solid/liquid interface.

Key reference:
D. P. Goronzy,
ASC Nano **12**
(2018), 7445.

video


WWW


Both conditions require the system to be close to thermodynamic equilibrium to suppress kinetic limitations (see box 10). In the thermodynamic equilibrium, the islands of the condensed molecular phase are in a dynamic equilibrium with their surroundings, i.e., free molecules that diffuse on the bare substrate. These molecules attach to existing islands at the same rate as other molecules detach. The self-assembled phases are therefore not stable *per se*, but the surrounding environment should always be considered.

One of the kinetic strategies to form long-range ordered organic or metal-organic networks is to prevent the formation of defective motifs. We have employed this strategy to build the metal-TCNQ networks on graphene (see Section 13) by controlled co-deposition of both components.

The attention of the field is now turning to on-surface reactions and on-surface synthesis to facilitate the synthesis of molecules and polymers that is not accessible in solution.⁸⁻¹⁰ Surface chemists explore new synthetic pathways different from chemical syntheses in solution or gas. Covalent polymerization on solid surfaces promises fabrication of polymers with

unique structures and properties, as demonstrated by the precise synthesis of graphene nanoribbons with defined width and edge geometry and functionalization. Polymerization reactions in the 2D confinement of a surface are fundamentally different from those in the bulk, solution, or gas phase environment. The surface confines monomers, intermediate oligomers, and polymers and provides an anisotropic surrounding with spatially defined reactive sites (a template). Also, in an often-used vacuum environment, the absence of solvents dramatically changes chemical reactions. While the major advantages of non-covalent self-assembly (i.e., efficient error correction and self-recognition) are missing, the high stability of the products outweighs the significant challenges connected to preparing long-range ordered covalent polymers with a minimum of defects. In this respect, pre-templating into self-assembled networks and non-thermal activation present a promising route here.¹¹

CONVERSATION

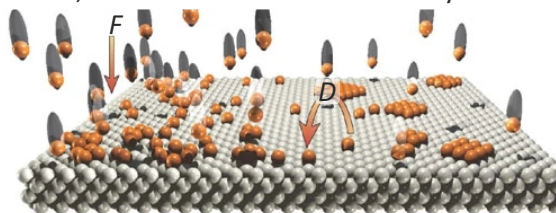
Pauli said: "God made the bulk;
surfaces were invented by devil"

Then, we do infernal investigations.

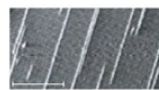
FEATURE

Kinetics vs. thermodynamics.

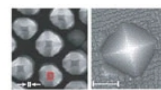
While thermodynamics determines the equilibrium structure, kinetics defines its accessibility.



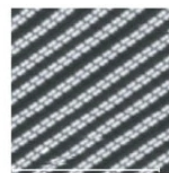
$\frac{D}{F}$ ← kinetics thermodynamics → $\frac{D}{F}$



Diffusion limited regime



Strain relaxation



Molecular self-assembly

During the growth, atoms/molecules are deposited from the vapor phase. When adsorbed, they diffuse on terraces to meet other adspecies, resulting in the nucleation of aggregates or attachment to already existing islands. The type of growth is determined by the ratio between diffusion rate D and deposition flux F . For large D/F , the resulting structure is close to the equilibrium one; for low D/F , metastable kinetically limited structures are obtained.

Key reference:

J. V. Barth et al.,
Nature **437**
(2005), 671.

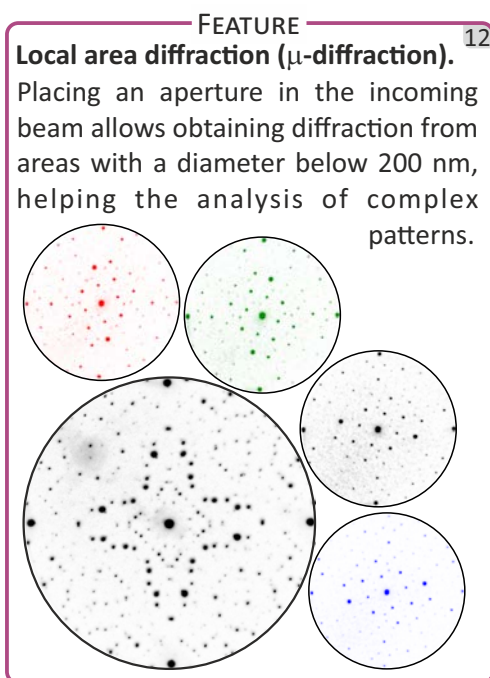
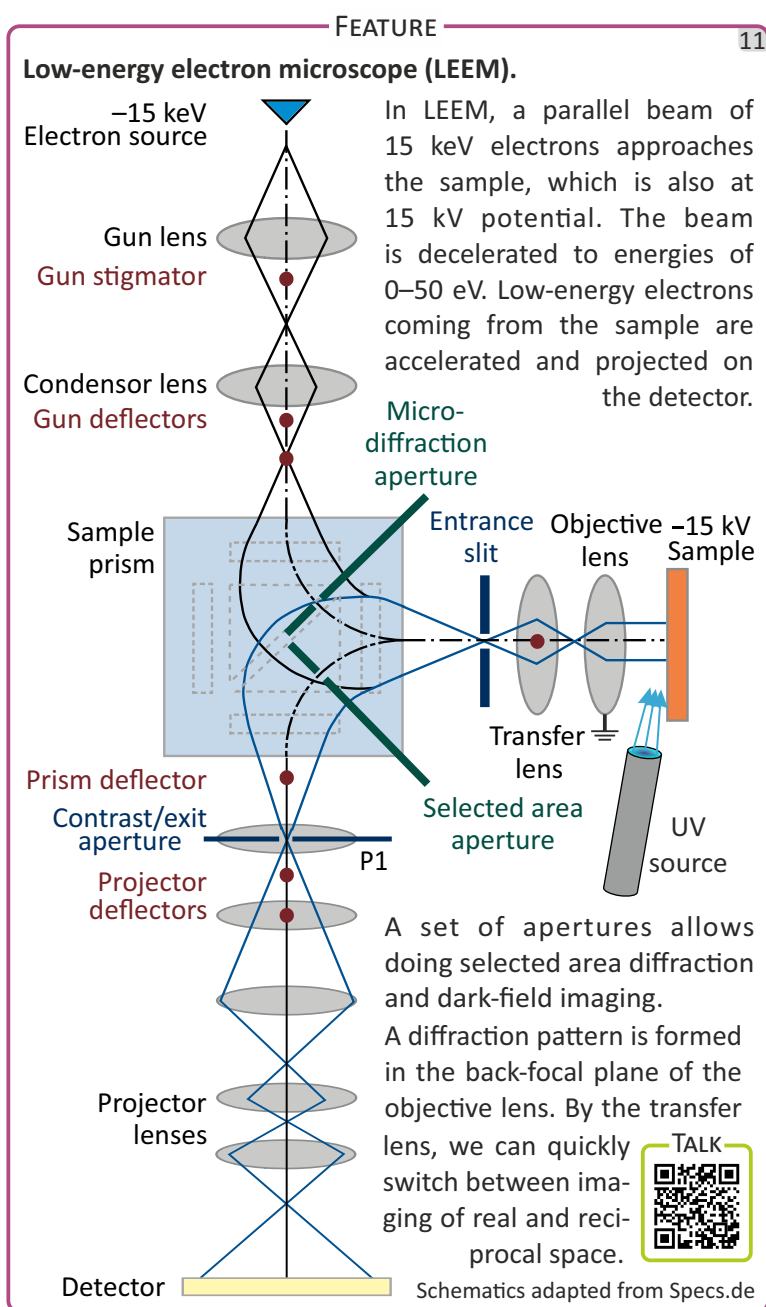


4 Low-Energy Electron Microscopy

Low-energy electron microscopy (LEEM, see box 11)¹² has quickly become the primary method in our research. LEEM images the sample in real-space at a mesoscopic scale (up to 15 μm) by low-energy electrons (0–50 eV) and also provides low-energy electron diffraction patterns. The measurement is reasonably fast; the first results come in minutes. Notably, the measurements can also be performed in real-time (typically 200 ms per frame) during sample annealing, irradiation, deposition of new material, or exposure to a specific gas, thus monitoring changes occurring in response to the treatment.

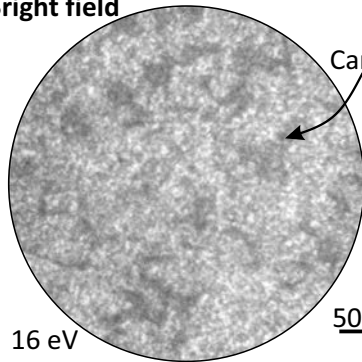
Low-energy electrons reflected/scattered from the sample provide several contrast mechanisms in the bright field images.¹³ These cover: (i) electric field inhomogeneities due to distinct surface morphology, differences in the local work function of various parts of the surface, and

the presence of contact potentials or magnetic fields; (ii) different scattering amplitude related to the different atomic structure of observed material; and (iii) Fresnel diffraction of reflected electrons, e.g., from the bottom and top areas around atomic steps on crystalline surfaces or due to multiple reflections in layers. These mechanisms enable us to follow changes in the structure and morphology of molecular phases described below.



Dark-field imaging.

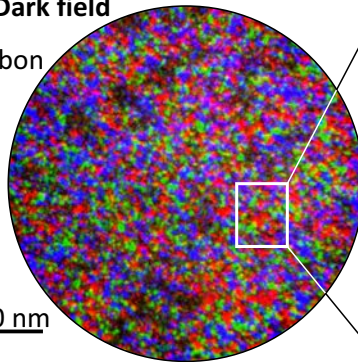
Imaging only the selected phase or orientation domain is done by blocking all scattered electrons except for a single selected diffracted beam by an aperture. Combined color-coded dark-field images provide the spatial distribution of phases or domains on the sample surface.

**Bright field**

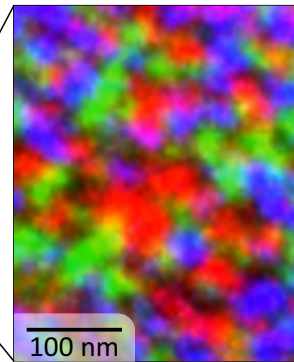
16 eV

Dark field

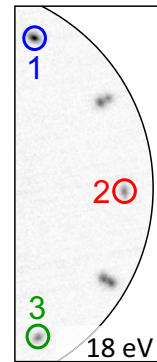
Carbon



500 nm



100 nm



1

2

3

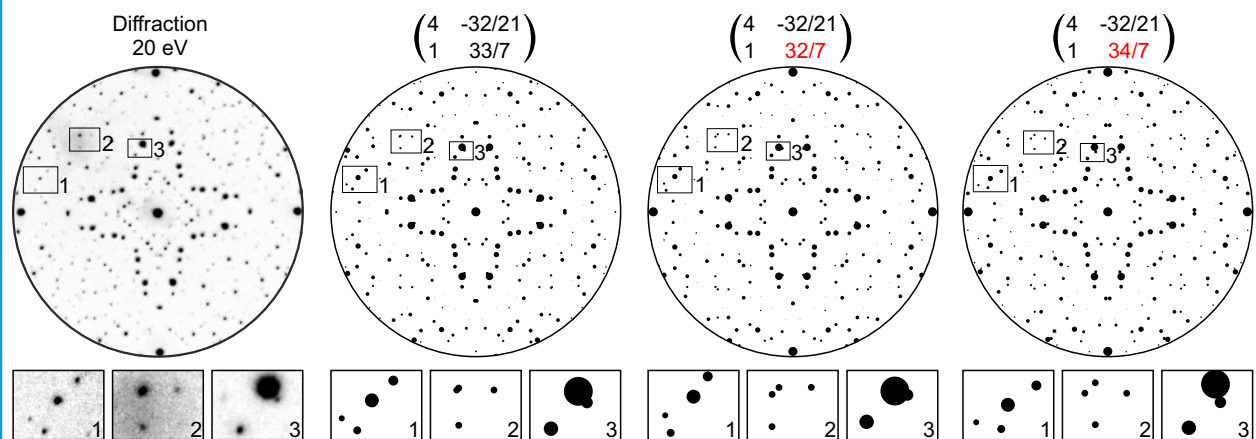
18 eV

Placing apertures into the electron beam enables advanced LEEM modes. Placing “microdiffraction” aperture spatially restricts the incoming electron beam allowing to measure the diffraction on areas with diameter going down to 185 nm (see box 12). In this way, we can measure diffraction only from a single molecular domain, helping disentangle complex diffraction patterns originating from multiple domains or phases. Conversely, multidomain diffraction patterns allow precise determination of unit-cell parameters by the local congruence method (see box 14). In dark-field imaging, we employ an aperture to obtain the distribution of phases or orientational domains on the surface (see box 13).

In our laboratory, LEEM gives us mesoscale information on the molecular phases, especially their formation and transformation during thermal annealing. In addition, the real-time capability is very useful: we stop the measurements and do STM and XPS (see the next section) when a new phase is formed and is the only one on the sample surface. The presence of a single phase is important especially for the area-integrated XPS measurements. STM helps to relate the distinct contrast in the LEEM images and the diffraction patterns with the molecular arrangements associated with the molecular phases. XPS then provides chemical information necessary for the interpretation of observed changes.

LOCAL CONGRUENCE METHOD

The mutual position of diffraction spots from differently oriented domains presents a very sensitive tool for obtaining the superstructure unit cells. Even small variation in the proposed model results in an observable discrepancy between the calculated and measured diffraction patterns.



5 Scanning Tunneling Microscopy and X-ray Photoelectron Spectroscopy

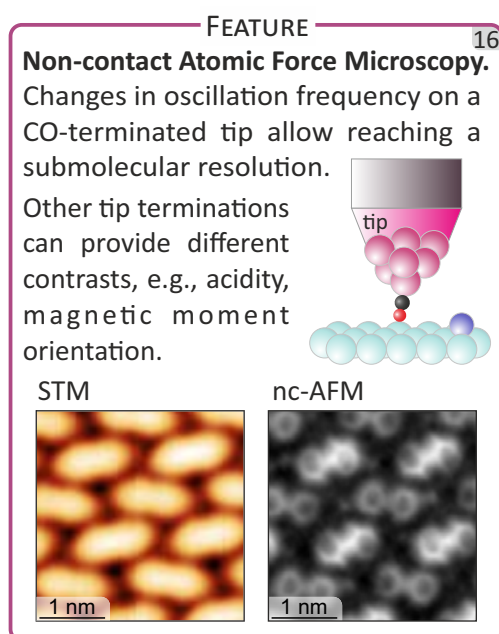
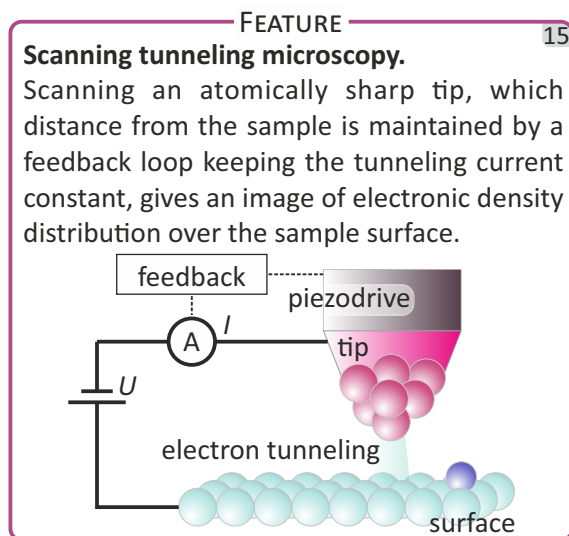
The discovery of STM revolutionized surface science. For the first time, observing the atomic structure of surfaces in real space became possible. The principle of STM is relatively simple: with an atomically sharp tip, we approach the surface of the studied sample to the distance where electron tunneling occurs (see box 15); the applied voltage leads to measurable tunneling current (30 pA–10 nA). Scanning by the tip over the surface then provides an atomically resolved image. Usually, the tip is maintained in a tunneling regime with a feedback loop regulating its distance from the surface to keep the tunneling current constant.

The tip should be atomically sharp, i.e., terminated by a single atom. The prepared tips, e.g., by electrochemical etching, are sputtered in UHV to remove the contaminants, e.g., a non-conductive oxide layer. But even freshly prepared tips are not guaranteed to be “good”, i.e., atomically sharp. A good tip is usually obtained by “working on the tip”, which covers various approaches. This covers the application of bias voltage pulses (up to 10 V), changes in bias voltage polarity, or on-purpose crashing the tip into the substrate. It takes a significant amount of time to get a good tip; if you have it, you rarely leave the lab.

By changing sample bias, we access distinct imaging contrast. If a positive sample bias (+) is applied, electrons tunnel from tip to sample, imaging the empty states; negative bias (–) means tunneling from sample to tip leading to imaging the occupied states.

It is important to remember that we use tunneling current as a probe. Therefore, we do not image topography but the local density of electronic states that is superimposed with topography. This fact is utilized in scanning tunneling spectroscopy: by measuring the derivative of the tunneling current dependence on the bias voltage (dI/dV), we obtain a spectrum of the density of electronic states. STM images of molecules usually do not show any internal structure because the density of states is delocalized over the molecules. For imaging of intramolecular structure, non-contact AFM can be employed (see box 16).

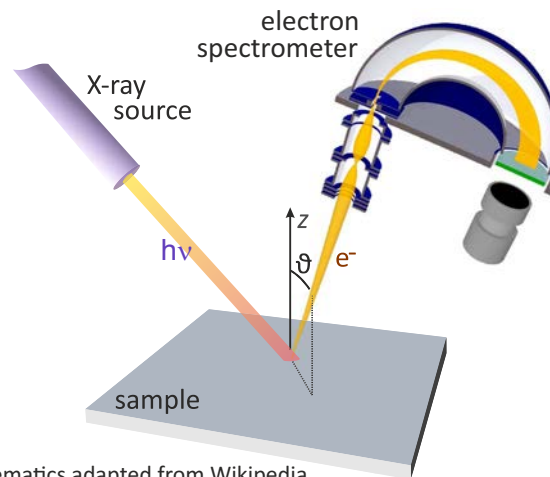
In our laboratory, STM provides information on the atomic-level structure and arrangement of molecules within the unit cell that complements LEEM data.



XPS provides a quantitative, bond-specific chemical composition of near-surface layers of studied samples (box 17). With an electron spectrometer, we measure the number of emitted electrons as a function of their kinetic energy from a sample irradiated with monochromatic X-rays, the photoelectron spectrum. The peaks in the photoelectron spectrum have positions characteristic to the elements from which they were emitted. However, the spectrum provides a wealth of information beyond the concentration of elements.

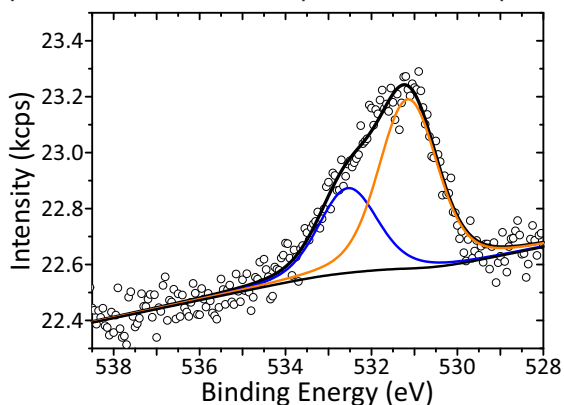
FEATURE 17
X-ray photoelectron spectroscopy (XPS).

Sample irradiation with X-rays causes the emission of photoelectrons. Their spectrum shows a set of peaks, reflecting the energy levels of atoms in the sample. As the position of the peaks is characteristic for each element, we obtain the chemical composition of the sample. From slight peak shifts, we learn about the bonding environment of atoms in the studied sample.

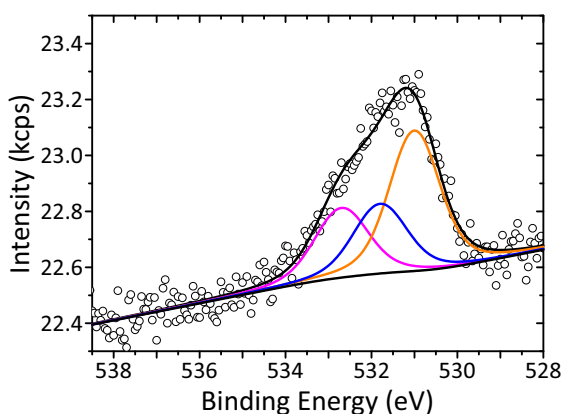


PEAK FITTING 18

Detailed information on the chemical environment can be obtained by fitting the measured spectra with components. Peak fitting follows strict rules imposed by physics but should also provide a realistic description of the sample.



The spectrum above can be fitted into 2 or 3 components with 1:2 or 1:1:2 intensity ratios. Both fits have the same quality, but the 2-peak one does not match with number of oxygen atoms (4) in the binding motif, whereas the 3-peak does.

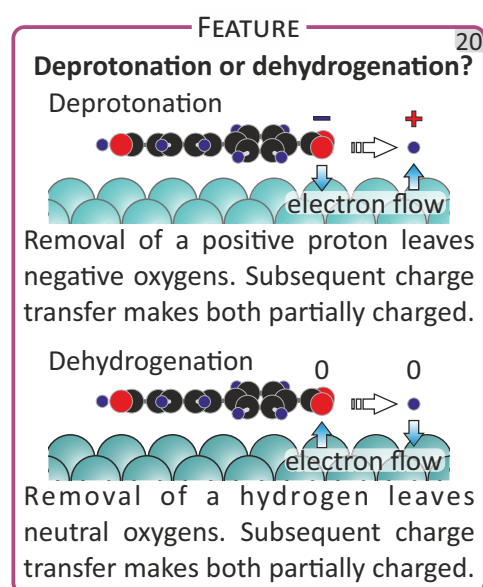
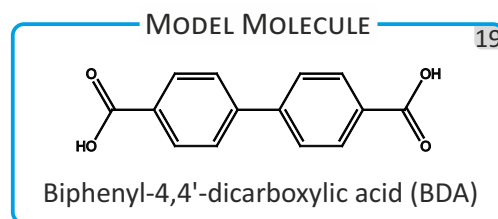


The peaks are slightly shifted (up to a few eV) depending on the chemical environment around the measured atoms. These shifts are usually identified in the detailed spectra by modeling the shape of the measured peaks by components, i.e., by fitting (see box 18). The shifts of the peaks are proportional to the charge transfer: if there is an electronic transfer to the measured atom, the peak shifts to lower binding energies and vice versa. However, we should note that photoemission is a quantum mechanical process and this simple rule is not always valid. Other features in the measured spectra also provide valuable information. For example, the shake-up peaks can be used to discriminate the spin configurations of studied atoms. The Auger peaks show different shifts than photoelectron ones and allow the determination of chemical states, which are not resolved in photoelectron peaks.

In our research, chemical information provided by XPS enables us to explain the changes in the studied molecular phases.

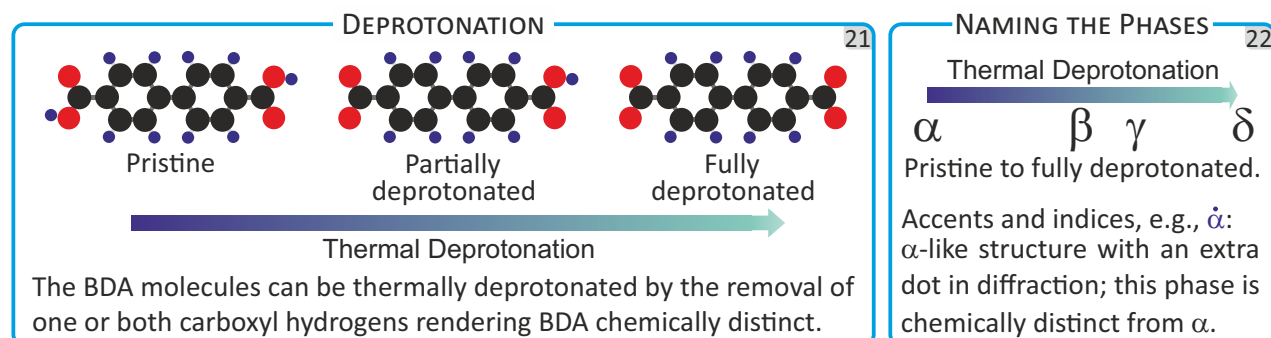
6 Thermal Deprotonation

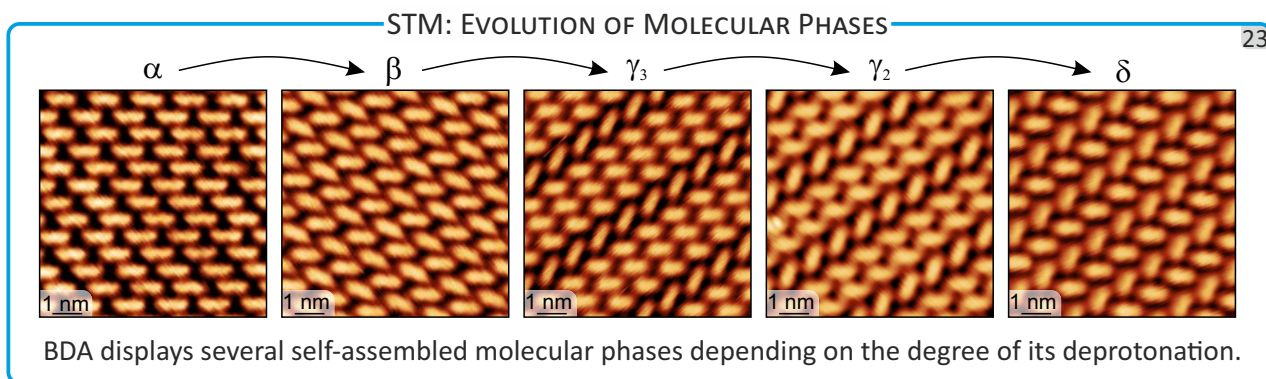
The following sections show different aspects of molecular self-assembly. For this, we employ a model system: biphenyl-4,4'-dicarboxylic acid (BDA, see box 19) on Ag(001) and Ag(111) substrates. BDA features two phenyl rings that impose its flat-laying geometry on metal surfaces, and two carboxylic end-groups that mediate intermolecular hydrogen bonds and enable the formation of extended supramolecular assemblies. These groups can be chemically transformed on Ag substrates: sample annealing to elevated temperatures leads to dehydrogenation (also called deprotonation, see box 20) – dissociation of hydrogen from carboxylic groups of BDA, which can be controlled by annealing temperature and time.



One or both carboxyl groups of BDA can be deprotonated (see box 21). As the thermal deprotonation proceeds, we obtain a series of molecular phases that comprise a mixture of pristine, semi-deprotonated (one of the BDA's carboxyl groups is deprotonated), and fully deprotonated BDA molecules with a given ratio. On Ag(001), the gradual deprotonation of a submonolayer coverage of BDA leads to the formation of multiple molecular phases that we refer to as α , β , γ_3 , γ_2 , and δ (see boxes 22 and 23); these phases have been thoroughly described in our papers.^{14–16} In the full layer, the α phase is formed instead of the β phase due to the spatial constriction. There are two distinct fully deprotonated phases, δ and ϵ . The δ phase is obtained by annealing above 400 K, whereas the ϵ phase is obtained only non-thermally, e.g., by e-beam irradiation.

These phases differ in the degree of deprotonation of carboxyl groups, i.e., α comprises only the pristine BDA with fully protonated groups, β , $\dot{\alpha}$, γ_3 phases comprise 50% of deprotonated groups, γ_2 phase 66%, and δ and ϵ phases 100%. The deprotonated carboxyl oxygens form chemical bonds with the substrate; the released hydrogen associatively desorbs from the surface, which is driven by a considerable decrease of the free energy of the system.¹⁷

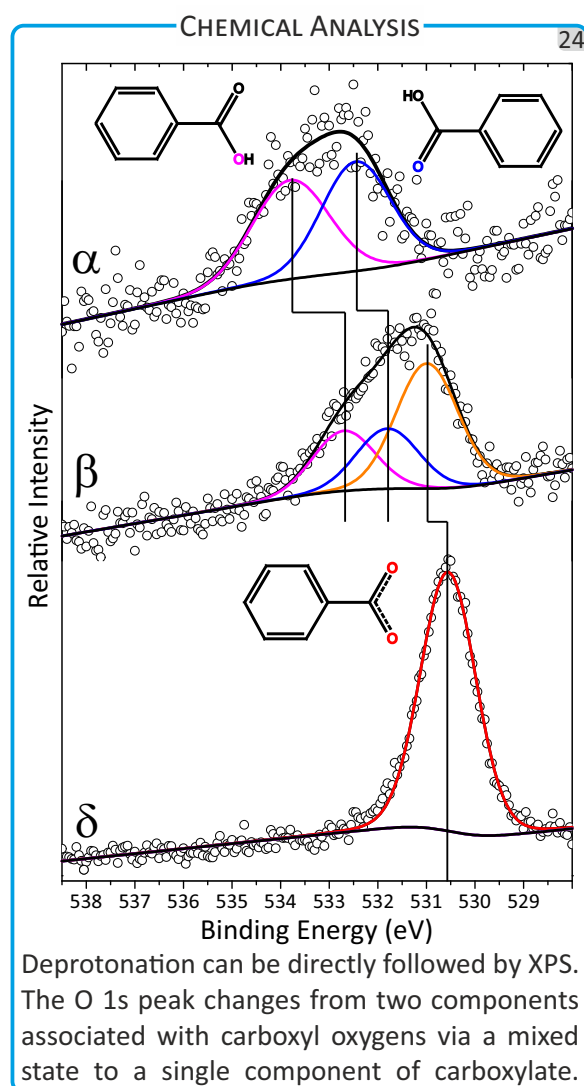




The degree of deprotonation can be followed by XPS (see box 24). Each of the three observed binding motifs has a characteristic spectral fingerprint. Complementary hydrogen-bonded carboxyl groups in the α phase manifest themselves by two peaks in the O 1s spectrum; the peaks with an intensity ratio close to 1:1 are associated with hydroxyl and carbonyl oxygens of the carboxyl group (see box 24). The α and β phases feature the carboxyl-carboxylate binding motif. In the O 1s spectrum, three peaks with 1:1:2 intensity ratio are associated with hydroxyl and carbonyl peaks of carboxyl and with two oxygen atoms of carboxylate. Finally, the carboxylate-phenyl motif shows a single peak for both carboxylate oxygen atoms.

The β phase displays a fixed degree of deprotonation in a broad temperature range, which points to hindered deprotonation within the β phase. Stabilizing the degree of deprotonation within condensed phases renders the BDA phases metastable, significantly influencing the transformation kinetics (see Section 8).

Each of these phases shows interesting features. The α phase represents an ordered phase that is non-periodic (see Section 9). The β phase is long-range ordered but disordered on a molecular level with a random distribution of pristine, semi-, and fully deprotonated BDA molecules. Thus, the β phase is a non-glassy disordered self-assembled phase. Finally, γ and δ phases represent k -uniform tilings (see Section 10).



READ ALSO

This topic is discussed also here:



KEY PUBLICATION

P. Procházka et al.: Phase Transformations in a Complete Monolayer of 4,4'-Biphenyl-Dicarboxylic Acid on Ag(001). *Appl. Surf. Sci.* **547** (2021), 149115.



7 Role of the Substrate

The substrate plays an essential role in molecular self-assembly: it is where molecular ordering takes place. Besides that, substrates provide a template for self-assembly, act as a source or sink for electrons during chemical reactions, and supply of adatoms. We should always consider the substrate to be a part of the system; in many cases it is not inert (box 25). If the adsorbed molecules chemisorb onto the substrate, they make

strong bonds and can be decomposed during this process. But even the inert substrate is a place where adsorption, diffusion, nucleation, and growth of self-assembled phases occur.

The ever-present effect of the substrate is templating. The substrate surface features a periodic lattice of atoms and the adsorbed molecules optimize their positions according to the potential landscape the substrate provides. The substrate symmetry (see box 26) defines the symmetry-equivalent positions of adsorbed molecules.

Another important role of the substrate is providing the adatoms, which can be incorporated into metal-organic networks¹⁸ or act as a reaction intermediate in coupling reactions. While we did not report it in our papers, annealing the samples comprising δ phases on Ag surfaces above 200 °C leads to decarboxylation of BDA, i.e., removal of its carboxylate groups, which is observed as the disappearance of O 1s peak in XPS spectra. In STM, we identify two kinds of chains (see box 27). The first consists of biphenyl biradicals alternating with Ag atoms, and the second one polyphenyl chains, in which the Ag adatoms were eliminated. The availability of adatoms depends on the substrate, and significant differences were observed in reaction kinetics of Ullmann coupling reaction on different substrates.¹⁹

CONVERSATION

Why do you use silver?

Gold is boring, copper is boring...

Boring? Why?

There is no deprotonation on gold.
And on copper everything happens below room temperature.

And other metals?

They destroy your molecule.

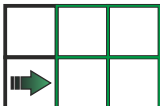
FEATURE 25

Substrates:
strongly interacting
transition metals
Cu
Ag
Au
graphene
weakly interacting


FEATURE 26


Isometry (congruence transformation): mapping in Euclidean plane E^2 onto itself that preserves all distances.


Symmetry of a set A : isometry σ which maps A onto itself ($\sigma A = A$).




Symmetry operations:

Translation: 

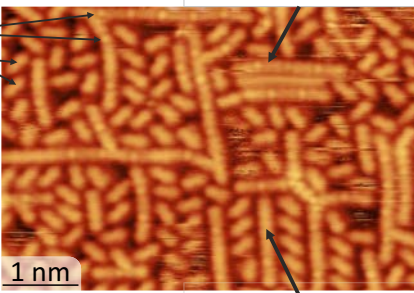
Reflection: 

Rotation: 

Glide reflection: 

FEATURE 27

Incorporation of substrate atoms: Substrate atoms can play the role of reaction intermediate, e.g., in decarboxylative homocoupling of BDA on Ag occurring above 200 °C.



[-biphenyl-Ag]_n reaction intermediate

↓

polyphenyl

Both intermolecular and molecule-substrate interactions play a significant role in the molecular self-assembly on the solid surface. In the case of planar aromatic molecules and an inert surface, a flat-lying adsorption geometry maximizes the contact area between molecules and substrate that are coupled predominantly by van der Waals interactions. The presence of functional groups dramatically changes both intermolecular and molecule-substrate interactions, which results in distinct molecular bonding patterns, changes of the substrate structure (reconstruction)^{20,21} and morphology (reshaping)^{22,23} (see box 28), or incorporation of substrate adatoms into bonding patterns²⁴.

Interactions with no analogs in the bulk or liquid may exist on the solid surface and have a dominant effect on the resulting structure.^{21,25,26} An interplay between molecule-molecule and molecule-substrate interactions turns out to be decisive for the resulting arrangement of the employed molecules. The term ‘subtle interplay’ expresses that even small changes in the substrate or molecule can cause substantial alterations in the resulting self-assembled structure.²⁷

This thesis is mainly dedicated to BDA on silver, but let us look at how it is on different substrates. The BDA deprotonation is significantly influenced by substrate material and surface plane orientation. On Cu(100), BDA forms a self-assembled structure consisting of fully deprotonated molecules already at room temperature.²⁸ On Cu(111), the situation is slightly different: a mixture of partially deprotonated and fully deprotonated phases appears on the surface at room temperature.²⁹ This indicates a lower reactivity of the (111) surface compared to the (100). However, in general, Cu has a considerably higher reactivity for deprotonation of BDA than Ag and Au. BDA on Ag(100) deprotonates very slowly at room temperature, and annealing at higher temperatures is necessary to reach a noticeable degree of deprotonation in a reasonable time. Concerning deprotonation, the Ag(111) surface is less reactive than Ag(100). No deprotonation of BDA on Au substrates has been observed.³⁰ Hence, the substrate material has a decisive role in the deprotonation of deposited carboxylic acids and surface plane orientation also affects the reactivity and structure of molecular phases.

FEATURE

28

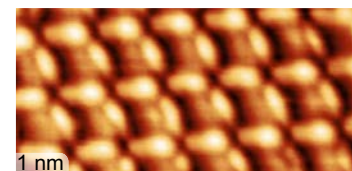
Shaping substrate surface.

Substrate is inherent part of the system.

Fully deprotonated BDA shapes substrate step edges to match the phase boundary.

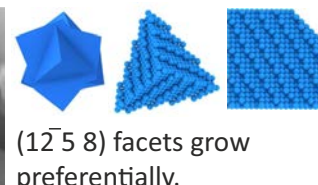
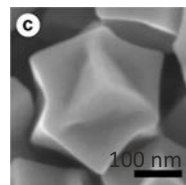


The metal-organic network shapes Ag(100) terraces to be 1 molecule wide.



Shaping gold nanocrystals.

L-Cys induces preferential growth of chiral facets during the growth of Au nanocrystals.



(12 $\bar{5}$ 8) facets grow preferentially.



Key reference:
F. Wu et al.,
Nano Lett. **22**
(2022), 2915.



READ ALSO

WWW



KEY PUBLICATION

A. Makoveev et al.: Role of Phase Stabilization and Surface Orientation in 4,4'-Biphenyl-Dicarboxylic Acid Self-Assembly and Transformation on Silver Substrates. *J. Phys. Chem. C.* **126** (2022), 9989.

WWW



8 Transformation Kinetics

BDA forms several molecular phases that appear with its increasing deprotonation. We can follow the transformation of one phase into the subsequent one in real space and real time by employing LEEM (see boxes 29 and 31). We use the term “transformation” to highlight that the presented phase transitions are irreversible. The irreversibility is a direct consequence of associative hydrogen desorption from the surface under UHV conditions.¹⁷ The extremely low hydrogen partial pressure in the surrounding environment causes the reverse process, i.e., dissociative hydrogen adsorption, to occur very rarely. Thermodynamically, this is expressed by a large free energy decrease of 0.5 eV per H atom associated with the entropy of desorption process.¹⁷

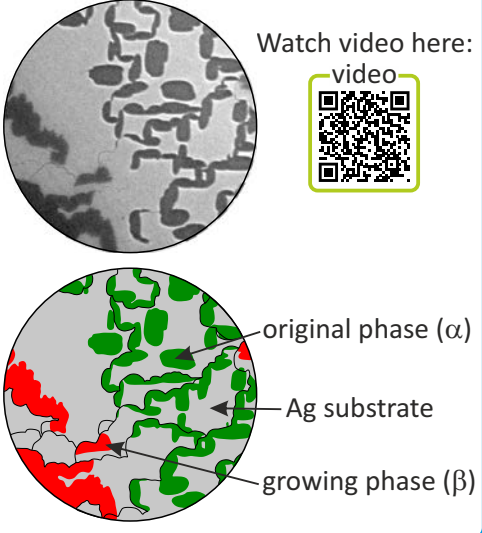

The video referenced in the box 29 shows the formation of β phase islands simultaneously at different locations within the LEEM view field. Once the first nuclei of the β phase islands appear, the $\alpha \rightarrow \beta$ transformation is relatively quick (about 40 seconds). When nucleated, the β phase islands grow at the expense of the α phase domains in a manner that we refer to as *remote dissolution*. Here, an expanding *capture zone* exists around each β phase island, and when this zone reaches the surrounding α phase islands, these quickly dissolve.

We have explained this behavior by a general growth-conversion-growth model validated by kinetic Monte Carlo simulations (see box 30). The transformation follows the La Meer burst nucleation mechanism, which we extended to the concept of “burst transformation”. Burst nucleation appears as a consequence of a large *critical nucleus size* due to a relatively weak intermolecular interactions.

VIEW ON PHASE TRANSFORMATION ²⁹

Video showing the remote dissolution of the α phase and its transformation into the β phase.

Watch video here:
video



Theoretical tools.

Density Functional Theory (DFT) provides the ground state configuration of the system.

In **molecular dynamics (MD)**, the vibrational motion of every atom around its equilibrium position is followed, visualizing thus the dynamic evolution of the system at short time scales.

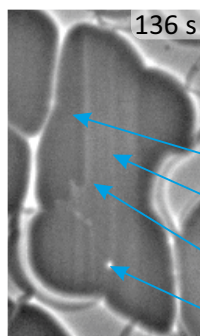
Kinetic Monte Carlo simulations (kMC) provide the dynamic evolution of the system. kMC focuses on the important events that correspond to the elementary reactions (adsorption, desorption, diffusion, or recombination), knowingly ignoring the description of all vibrations, thus enabling longer simulation times.

The molecular phases are in a dynamic equilibrium with the corresponding 2D gas of BDA molecules diffusing over the surface. The 2D gas plays an indispensable role in the phase transformations: it mediates mass transport between the individual islands and hosts deprotonation reaction. While deprotonation also occurs within the condensed phase, the intermolecular bonds stabilize the initial state, which increases the activation energy for deprotonation. Therefore the deprotonation is much faster in 2D gas than in the condensed phase.

INTERNAL TRANSFORMATION

31

If two phases possess a similar structure, the phase transformation can proceed internally, i.e., within existing molecular islands. Watch video here:



video
growing phase (γ)
original phase (β)
transformation front
void in mol. island



We have observed different kinds of phase transformations between BDA phases on Ag(001). The $\alpha \rightarrow \beta$ transformation can be assigned to a first-order transition. The structure of the growing phase (β) is incompatible with that of the previous phase (α). Therefore, the islands of the β phase nucleate outside the α islands. The situation changes for transformations between the γ phases. The structure of the γ phases shares the structure of one side of their unit cells. Hence, a new phase can grow on the periphery of the previous one. The transformation between the γ phases then proceeds locally within the voids propagating through the molecular islands or at the island

periphery; however, the overall shape and position of the islands are maintained (see box 31). In contrast, the $\alpha \rightarrow \tilde{\alpha}$ transformation is gradual and, hence, can be termed a second-order irreversible transition.

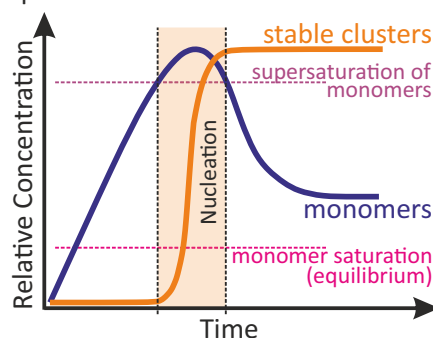
The general picture of burst transformation is as follows. At the beginning, there are islands of the initial phase in equilibrium with 2D molecular gas. With the steady temperature increase, more molecules are released to the 2D gas, where they can deprotonate. This gradually builds up the 2D molecular gas, and continuing deprotonation makes its composition different from the parent phase. The equilibrium condition requires more molecules to be detached and eventually deprotonated. At some point, sufficient supersaturation allows the formation of the new phase – its formation follows the La Mer burst nucleation mechanism (see box 32). The presence of islands rapidly decreases the supersaturation: the molecules from the 2D gas are attached to the newly nucleated islands. This has two effects: (i) without significant supersaturation, no additional nucleation occurs, and (ii) many molecules are released from the preceding phase, rapidly deprotonating and incorporated into new phase islands. This process, i.e., remote dissolution, continues until the islands of the initial phase are dissolved.

FEATURE

32

Burst Nucleation (BN).

A significant supersaturation has to be reached before the nucleation starts. Once reached, the nucleation events appear quasi-simultaneously. When the stable islands are present, the precursor molecules attach to them, decreasing the supersaturation below the point where nucleation can occur. Consequently, only the existing islands grow, and no further nucleation is possible.



Key reference:

A. Baronov et al.,
Phys. Chem. Chem. Phys.
17 (2015), 20846.



READ ALSO

This topic is discussed also here:



KEY PUBLICATION

P. Procházka et al.: Multiscale Analysis of Phase Transformations in Self-Assembled Layers of 4,4'-Biphenyl Dicarboxylic Acid on the Ag(001) Surface. *ACS Nano* **14** (2020), 7269.

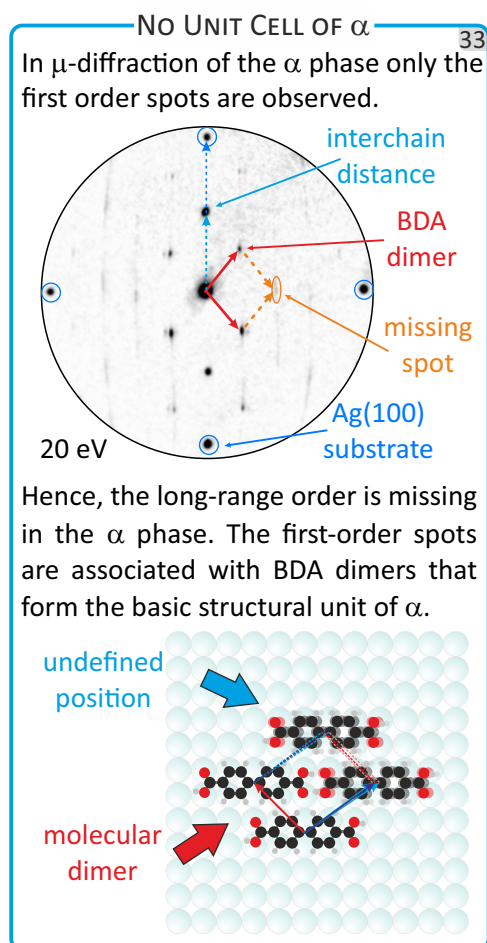
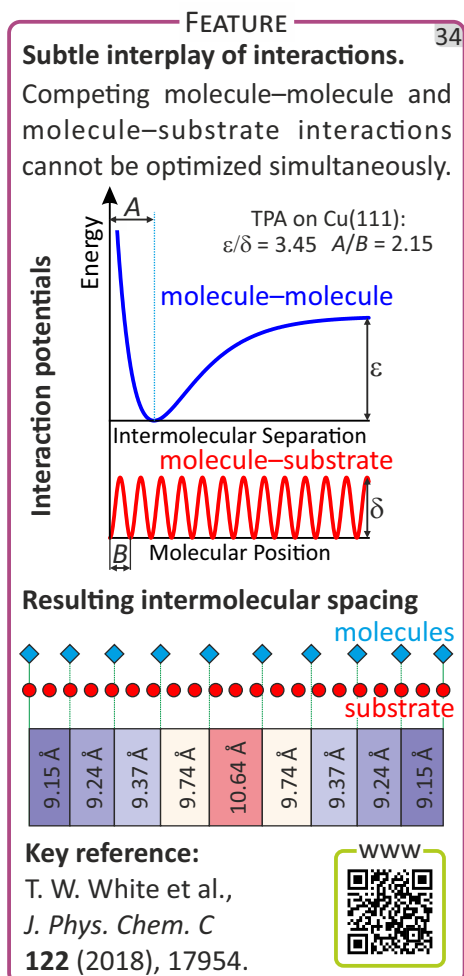


9 No unit cell of the α phase

Atomic and molecular phases usually show long-range order unless they are amorphous. BDA molecular phases do not differ from this concept except for the α phase.

The α phase is always difficult to describe in our manuscripts. It is relatively easy to describe the other phases both on Ag(001) and Ag(111) substrates because they are periodic and commensurate with the substrate (sometimes with a large superlattice; cf. local congruence method, Section 4). But for the α phase, there is no long-range periodicity, even if it looks periodic. It is hard to admit that we cannot assign any unit cell to the α phase (see box 33).

A periodic gas-phase arrangement of BDA on a periodic substrate produces a non-periodic structure. How is that possible? If we place BDA molecules on the substrate, their intermolecular separation and position with respect to the substrate cannot be optimized simultaneously (see box 34).



The BDA α phase comprises molecular chains of fully protonated molecules. Within these chains, the carboxyl groups of neighboring BDA form complementary hydrogen bonds. The BDA molecules are not spaced regularly but are shifted from “optimal” positions within the chain by ± 0.4 Å to enhance the binding with the substrate at the expense of increased energy associated with hydrogen-bond length change, as previously discussed for a relevant system comprising non-deprotonated TPA on a Cu substrate.²⁷

Upon deprotonation, the α phase is formed. It is structurally close to the α phase, but the matching with the substrate by the strong binding of carboxylate oxygen atoms to the substrate results in the appearance of intra-chain periodicity. Here, 5 BDA chain match 24 substrate atoms. However, these five molecules are also not placed regularly. In contrast, BDA in the α phase is only weakly van-der-Waals bonded to the Ag substrate.

Without anchoring points, the periodicity does not appear. In this situation, we obtain a system not listed in textbooks (see box 35).³¹ In this system, the competition of the molecule–molecule and molecule–substrate bonding results in an aperiodic molecular overlayer even though both molecular layer and substrate are periodic systems *per se*.

In contrast to Ag(001) substrate, the α phase on Ag(111) is periodic within the molecular chains. However, compared to Ag(001), where the interchain periodicity exactly matched the 2-substrate-atom distance, the Ag(111) surface is more densely packed. Therefore, the molecular rows no longer precisely fit the substrate, which results in a slight variation of the inter-row periodicity.

FEATURE 35

Superlattices: what is in textbooks?

Superlattice: lattice of different periodicity in the topmost (adsorbate) layer superimposed on the substrate lattice with the basic periodicity.

Simple superlattice
 $b/a = 2$

Coincidence lattice
 $b/a = 4/3$
lattices are commensurate

Incoherent lattice
 $b/a = 1.49953\dots$
lattices are incommensurate

MOLECULAR STRUCTURE AS TILING 36

The neighboring rows in the α phase can be arranged in two equivalent positions. We assign a tile to each configuration of 4 neighboring BDA molecules.

Employing these tiles, we obtain tiling that represents the α phase. The rectangle tile represents an average unit cell; the kite represents a twin domain boundary.

The interchain motif comprises a pair of BDA molecules in the neighboring chains (BDA dimers, box 33), which give rise to characteristic α -phase diffraction spots. However, there are two symmetry-equivalent positions for BDA molecules in the neighboring chains (see box 36). The existence of these possibilities results in a random sequence of chains.

In standard representation, the α phase unit cell can be expressed in matrix notation as $\begin{pmatrix} 24 & 0 \\ 2 & 2 \end{pmatrix}$. However, in this case, every change in the placement of the following molecular chain is associated with the twin boundary.

To better rationalize the structure of the α and α' phases, we can associate these two possibilities with two distinct tiles (see the next section): “rectangle” and “kite” (see box 36). In this representation, the rectangle tile represents an average unit cell and the kite a twin-domain boundary.

READ ALSO

This topic is discussed also here:



KEY PUBLICATION

P. Procházka et al.: Phase Transformations in a Complete Monolayer of 4,4'-Biphenyl-Dicarboxylic Acid on Ag(001). *Appl. Surf. Sci.* **547** (2021), 149115.



10 Tilings

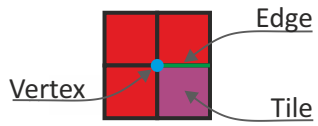
The division of a plane into regular polygons has fascinated people since ancient times. Many monuments are decorated with simple geometric objects forming complicated ornaments on murals or pavements across different cultures. The first rigorous mathematical treatment of tessellation of the Euclidean plane into regular polygons – tiles – was done by Johannes Kepler in his famous work *Harmonices Mundi*, “The Harmony of the World”.³² This famous set of 5 books introduced a mathematical description of planetary motion in the heliocentric system – Kepler’s Third Law. Surprisingly for many of his successors, a significant part of *Harmonices Mundi* was dedicated to tilings; in some transcriptions, these parts were shortened or even dismissed. Only in the 20th century, there was a renewed interest in tilings, as described in the excellent book by Grünbaum and Shephard.³³

There are only three ways of forming regular tilings as there are strict mathematical criteria defining regular tiling by *flag transitivity*.³³ If we relax the condition of a single type of tiles, we get additional eight semiregular or Archimedean tilings (see boxes 37 and 38). In these tilings, the vertices – joints of tiles – are all equivalent; mathematically, the Archimedean tilings are defined by the condition of vertex isogonality by the symmetry of tiling.³³ And if we allow more than one type of vertex, we obtain uniform tilings.

Tilings by regular polygons are of particular interest as they appear to be an extremal solution to various physical problems.³³ The introduction of a few new tiles into a certain tiling may profoundly alter its nature, which may be regarded as an analogue of the physical effects of introducing foreign atoms into a crystal. In this respect, the supramolecular rhombus tilings, which provided insights into the physics of dynamically arrested systems and the role of entropy in the balance between order and randomness in molecular phases, serve as an illustrative example.^{34–36} Tilings thus present intriguing model systems for complex physical problems.

FEATURE 37

Tilings: vertices, edges, and tiles



Tiling T is a countable family of closed sets $T = \{T_1, T_2, \dots\}$ which covers the plane without gaps and overlaps.


Symmetry S of the tiling T : isometry mapping every tile of T onto tile of T .

Uniform tiling: group $S(T)$ contains operations that maps every vertex of tiling T onto another vertex of T .

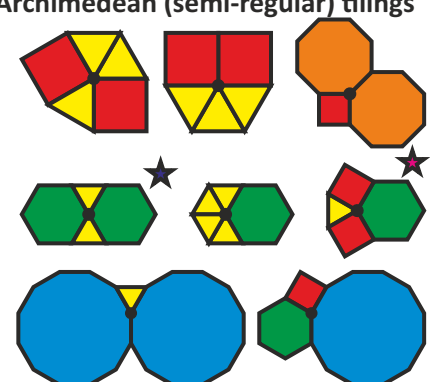
k -uniform tiling: edge-to-edge tiling which vertices form precisely k transitivity classes with respect to $S(T)$.

FEATURE 38

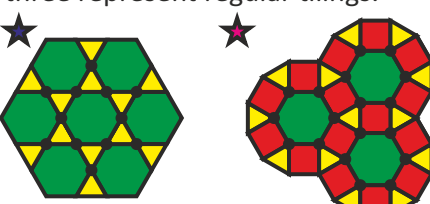
Regular Tilings



Archimedean (semi-regular) tilings

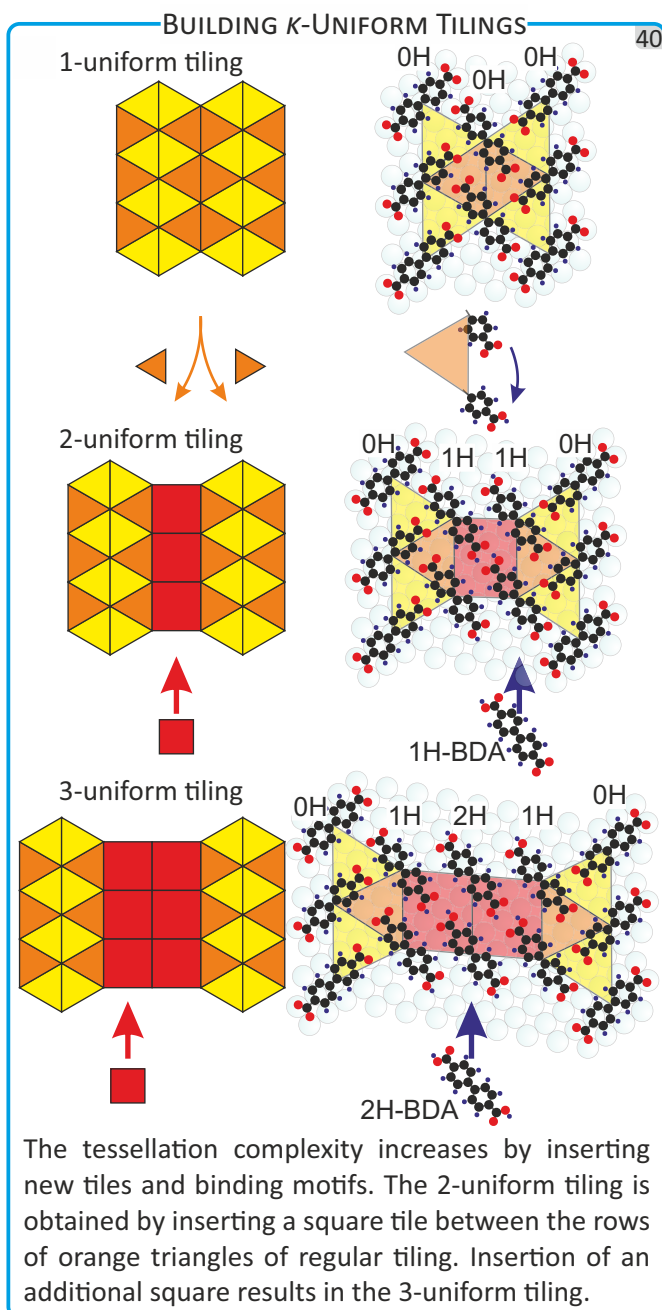
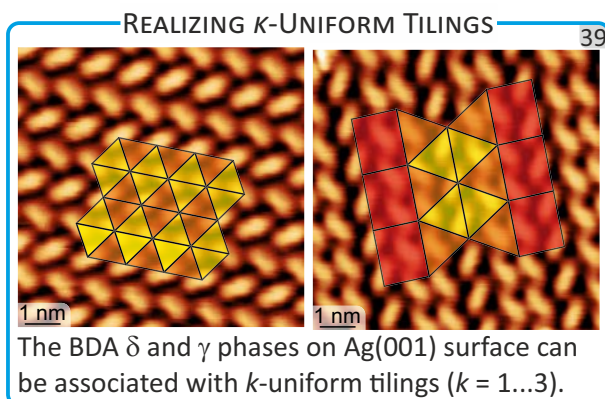


Vertices (joints of regular polygons) of 11 Archimedean tilings; the first three represent regular tilings.



Example of expression of tiling from vertices marked by an asterisk above. In Archimedean tilings, all the vertices are equivalent.

Experimental realization of complex surface tessellations on an atomic and molecular level thus enables exploring properties and utilization of these systems. In this respect, supramolecular chemistry offers tools for engineering self-assembled surface geometries expressing semiregular,³⁷⁻³⁹ fractal,^{40,41} quasicrystalline,^{42,43} and random³⁴ tilings.



We have found that BDA γ and δ phases on Ag(001) substrate can be associated with k -uniform tilings (see boxes 39 and 40).

Nature tends to produce simple structures. So, a single component system usually forms a regular or a semiregular tiling. Even putting together multiple components results in simple structures or segregation of components into two separate phases. Hence, the task is to combine two distinct phases with characteristic binding motifs; this can be realized using BDA. Deprotonation of only one of two carboxyl groups produces a bifunctional molecule that enables us to combine two binding motifs characteristic of two distinct pure phases. So, employing it together with intact and fully deprotonated BDA, we obtain a structure showing several types of vertices, i.e., a representation of a 2- or 3-uniform tiling. Box 40 shows how the tiling complexity increases with additional rows of molecules.

However, it is not only the right mixture of intact, semi-, and fully deprotonated BDA that defines tiling, but also a substrate geometry. On Ag(111), we observe structures with different geometry than that of k -uniform tilings.

BLOG POST

Read our blog post "Kepler would love it".



KEY PUBLICATION

L. Kormoš et al.: Complex k -Uniform Tilings by a Simple Bitopic Precursor Self-Assembled on Ag(001) Surface. *Nat. Commun.* **11** (2020), 1856.



11 Electron-Beam Induced Transformations

The temperature has a prominent position in natural sciences: many reactions and processes are thermally activated following the Arrhenius law. In self-assembly, thermodynamics usually defines the equilibrium structure, but also the kinetics of the involved on-surface processes, i.e., reaction rate, on-surface diffusion, nucleation, and growth, plays a crucial role. The kinetic rates of all the involved processes are generally thermally activated following the Boltzmann distribution and display a particular hierarchy of activation energies. With an increasing temperature, the rate of all the temperature-activated processes increases exponentially, with activation energies being the defining parameter (see box 41). The correct choice of temperature enables the adjustment of the rate of structural

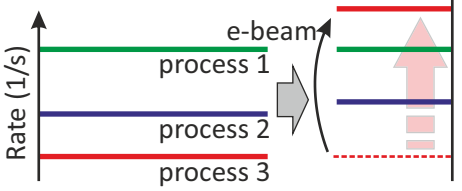
and chemical transformations to reach the desired product.⁹ However, this approach is not generally applicable because the hierarchy of activation energies cannot be easily rearranged.

The non-thermal activation methods⁹ present an alternative that circumvents this limitation. Photons and low-energy electrons can excite specific vibrational modes, access many reaction channels, deliver much higher energies, and excite plasmons for plasmon-induced chemical reactions. Electron-beam-induced reactions such as crosslinking/breaking polymer chains in electron beam lithography,⁴⁴ or precursor decomposition in electron-beam-induced deposition (EBID)⁴⁵ are the key technologies for nanofabrication. The commonly used high-energy-electron beams deliver too high energy densities, causing an extensive damage to adsorbed molecular layers, substantially reducing reaction selectivity.⁴⁶ Even low-energy (< 20 eV) electrons are still considered rather more damaging than useful, especially for organic adsorbates.⁴⁶

During our given oral presentations that include LEEM, we are usually asked if the electron beam influences the BDA molecules. It does. The e-beam irradiation of the α phase leads to the formation of new molecular phases. Depending on the electron energy, the ϵ phase is either formed directly or via the intermediate β phase. Whereas the formation of the β phase can be induced both by irradiation and thermal annealing above 340 K, the ϵ phase is only reached by e-beam irradiation.

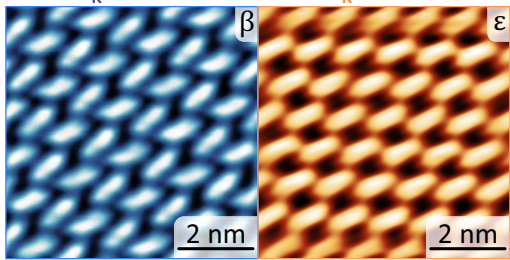
This result demonstrates the principle of kinetic structural control, i.e., the formation of distinct periodic structures as a function of the external parameter.

FEATURE ⁴¹
Thermally activated processes (TAPs).
In complex reactions, a TAP with the highest activation energy (E_A) is rate-limiting, i.e., defines the overall kinetics. All the rates increase with rising temperature T as $\exp(-E_A/kT)$. The specific hierarchy of E_A cannot be easily rearranged. Here, non-thermal activation methods can enhance the particular rate, changing thus the rate-limiting process.



ENERGY DEPENDENT STRUCTURE ⁴²
The e-beam irradiation of BDA/Ag leads to the formation of new molecular phases. Below 10 eV, the β phase grows first, followed by the ϵ phase. Above 10 eV, the ϵ phase grows directly. This hints at a change in kinetics when an e-beam of higher energy is used.

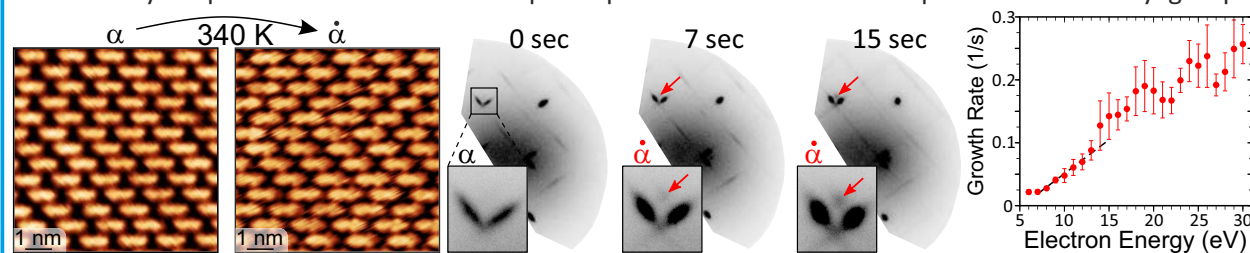
$E_k < 10$ eV $E_k > 10$ eV



KINETICS FROM DIFFRACTION

43

The transformation of the α phase requires only minor shifts of BDA within the existing structure. Hence, the intensity of spots associated with the $\dot{\alpha}$ phase provides the fraction of deprotonated carboxyl groups.

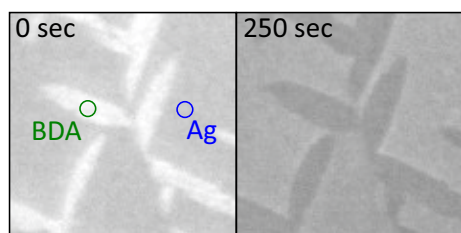


We have determined the deprotonation rate as a function of electron beam energy from the evolution of the intensity of the diffraction spots associated with the $\dot{\alpha}$ phase (see box 43). The $\alpha \rightarrow \dot{\alpha}$ phase transformation proceeds internally and features the formation of a carboxylate-substrate bond, which requires only minor vertical and horizontal shifts of BDA within the existing structure. Employing this phase transformation thus circumvents the complications encountered when the formation of the new phase includes on-surface transport, nucleation of deprotonated molecules and subsequent growth of the phases themselves. The growth rate of the $\dot{\alpha}$ phase increases with an e-beam energy above the threshold of 6 eV. We also tried to determine the deprotonation kinetics from the change in the reflected electron beam intensity of BDA islands in the bright-field LEEM images, but we failed (see box 44).

BRIGHT FIELD: SOMETHING ELSE

44

While we also observe changes in the contrast of BDA molecular islands in the bright-field LEEM images at the same time scale, we found that these changes are not directly proportional to degree of the deprotonation of BDA.



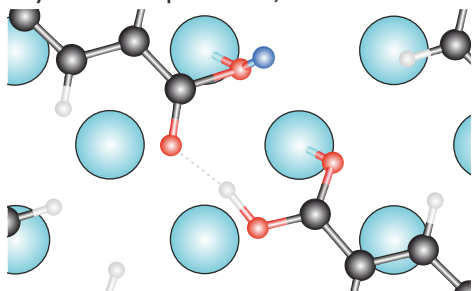
The growth of distinct phases depending on the e-beam energy is a direct consequence of the increased deprotonation rate of BDA. Depending on its competition/cooperation with the nucleation rate, either the intermediate β phase or directly the final ϵ phase is formed. A regulation of the deprotonation rate thus allows a change of the limiting factor from the rate of supply of the deprotonated molecules to nucleation of the molecular phase. Hence, selective enhancement of a process outside the ladder of activation energies that defines the deprotonation-nucleation-growth kinetics can be employed to obtain different products.

FEATURE

45

Deprotonation on metal surfaces.

In this process, a proton is extracted from carboxylic oxygen. The oxygen subsequently binds to the surface atom. The extracted proton (blue) stays near its parent O, until it desorbs.



The main interaction mechanisms of low-energy electrons with molecular layers are non-resonant electron impact ionization and electron impact excitation or resonant electron attachment.⁴⁷ As we do not see any clear signatures of resonance peaks, we associate the monotonic increase of the reaction rate above 6 eV with the non-resonant electron impact excitation process.

KEY PUBLICATION

A. Makoveev, et al.: Kinetic Control of Self-Assembly Using a Low-Energy Electron Beam. *Appl. Surf. Sci.* **600** (2022), 154106.

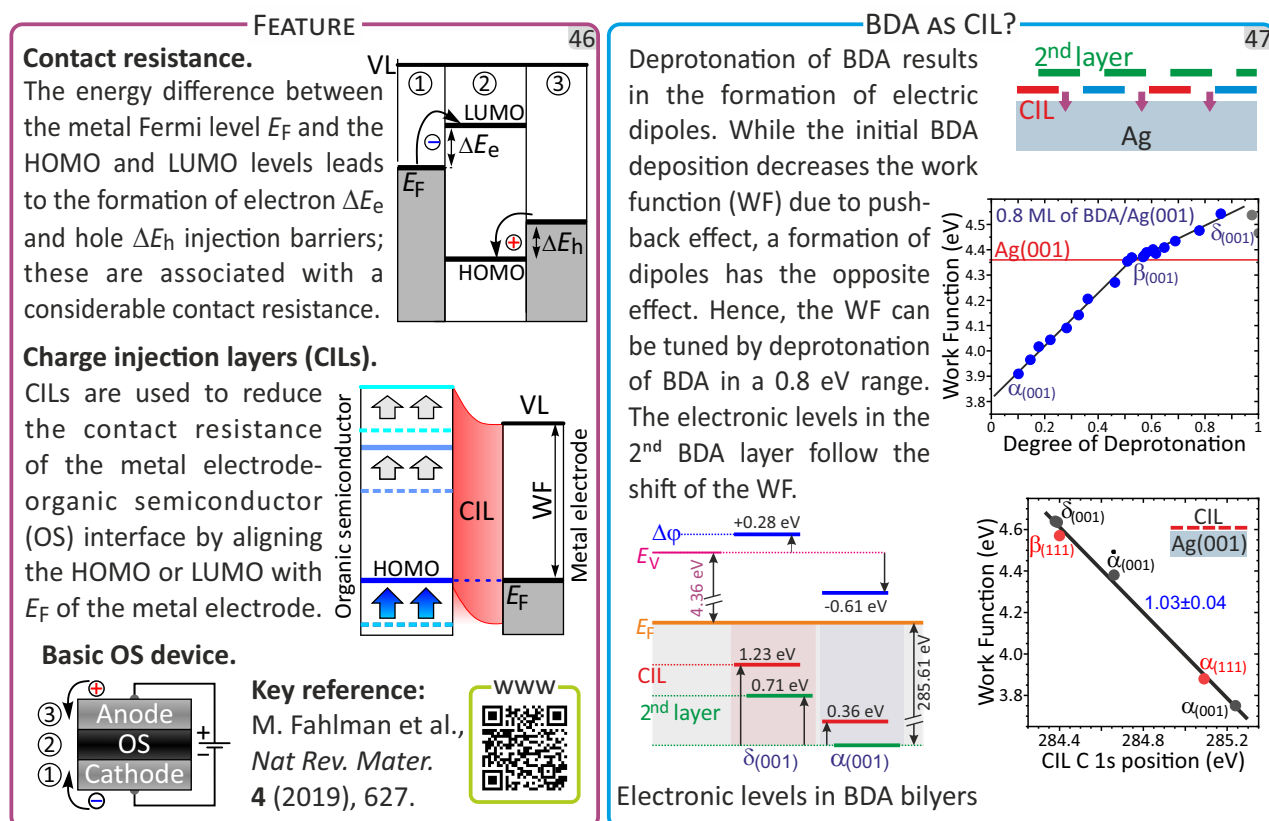


12 Vision: Organic Electronics

Facing the physical limits of the current semiconductor technology, several novel concepts are introduced to maintain the trends in the enhancement of operating speed, downsizing the individual transistors, and keeping the production costs. Simultaneously with high-performance transistors, devices with distinct functionalities, i.e., for sensing, energy harvesting, and illumination, were developed. Organic semiconductors (OSs) became an integral part of these devices as they aim at different applications employing transparent, flexible, and biocompatible materials and offer low-cost/high throughput processing.⁴⁸ To this end, OLED displays rule the market of high-end screens of mobile devices, organic photovoltaic cells are at the edge of large-scale commercial production, while organic thin-film transistors are still behind those above but with a range of promising demonstrations. OSs also offer a large degree of tunability in their mechanical, electrical, and optical properties over their inorganic counterparts, which can be used to add multifunctionality to a single device.⁴⁸

The interface between the OS and the metallic contacts defines the alignment of the molecular orbital levels of the OS with vacuum and Fermi levels of the metal. The alignment determines the electron and hole injection efficiency; a considerable contact resistance arises from energy level misalignment (see box 46).⁴⁸ The high contact resistance limits the operation frequency and restricts high current devices such as organic field-effect transistors.⁴⁸

One of the possibilities to reduce the contact resistance is to passivate the metal electrode by a thin insulating layer and establish the energy level alignment through integer charge transfer via the tunneling barrier.⁴⁹ However, tunneling contact is also associated with considerable contact resistance and energy losses despite the precise alignment.⁵⁰



FEATURE

48

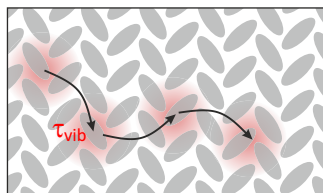
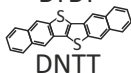
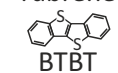
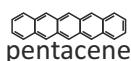
Organic semiconductors (OS).

High-mobility OSs (examples below) display room-temperature mobilities in the range $\mu \approx 1\text{--}20 \text{ cm}^2 \text{ V}^{-1} \text{ s}^{-1}$.

Transient localization model.

Charge carrier mobility $\mu = \frac{e}{k_B T} \frac{L^2}{2\tau_{\text{vib}}}$

Dynamic disorder due to intermolecular phonon modes causes a transient localization of carriers over a length L within a fluctuation time τ .

**Key reference:**

S. Fratini et al.,
Nat. Mater.
19 (2020), 491.



Therefore, the direct contact of molecules is preferable. In this case, the contact resistance can be decreased by so-called charge injection layers (CILs, see box 46) that reduce the energy level misalignment and, thus, increase the efficiency of OS-based devices.^{51,52}

Our approach uses BDA as a tunable single-layer molecular CIL (see box 47). When deprotonated, the carboxylate group possesses a partial negative charge, forming an interfacial dipole. By gradual deprotonation, we can prepare a range of molecular phases with a distinct density of dipoles $n_{\text{Dip}} = 2\mathcal{D}n_{\text{BDA}}$, where \mathcal{D} is the degree of BDA deprotonation and n_{BDA} is the surface density of BDA molecules each having 2 carboxyl groups. Deposited molecules induce the *pushback effect* that initially decreases the work function (WF).⁵³ The deprotonated carboxyl groups display a negative charge localized on the O atoms, which results in the formation of interface and intramolecular dipoles that

increase the WF by up to 0.8 eV. Along with the WF change, the energy levels of BDA in the second molecular layer shift accordingly. Following this initial success, we turn our focus on the systems comprising high-mobility OS (see box 48) deposited on the CIL, which are formed by various organic carboxylic acid molecules to lower the OS-electrode contact resistance.

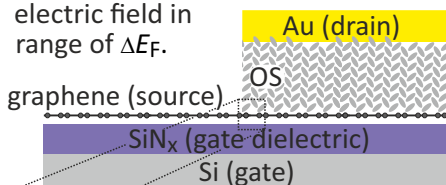
In a separate project, we aim to investigate the growth of OSs on graphene as a part of a vertical field-effect transistor (VFET, see box 49). The concept of a VFET device brings several advantages, e.g., high driving current, high-speed operation, flexibility, scalability and 3D integration, and compatibility with organic materials, while they are less demanding for lithographic processes.⁵⁴ In VFET, the semiconducting channel is sandwiched between source and drain electrodes; hence, its length is given by the semiconductor layer thickness.

FEATURE

49

Vertical field-effect transistor (VFET).

In VFET, the semiconducting channel is sandwiched between source and drain electrodes. Employing graphene as a gateable electrode enables modulating the Schottky barrier height at the graphene/OS interface by a gate electric field in range of ΔE_F .

**Key reference:**

L. Liu et al.,
Sci. China Inf. Sci.
63 (2020), 201401.



One of the VFET designs is the variable barrier interface transistor (barristor) employing graphene as a gateable electrode to modulate the Schottky barrier height at the graphene/semiconductor interface by the gate electric field.⁵⁴ In this way, the carrier transport through the device is controlled, and a large ON/OFF ratio can be achieved. In this project, we will focus on the formation of the graphene-OS interface and lowering the contact resistance, which still dominates the realized VFET devices.

KEY PUBLICATION

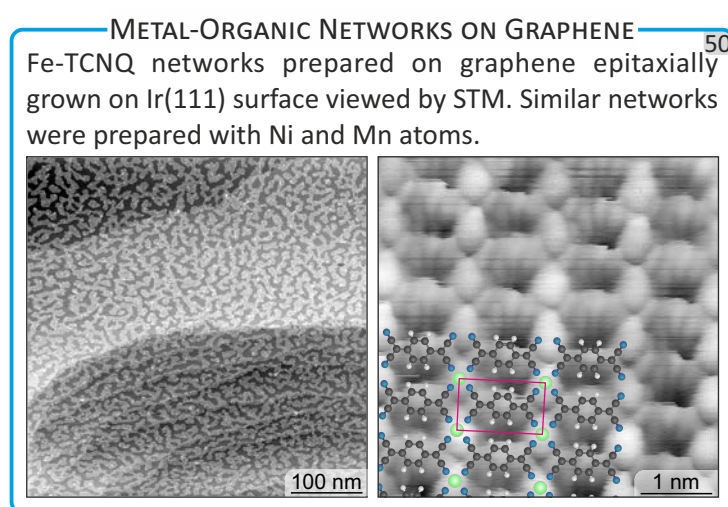
V. Stará, et al.: Tunable Energy Level Alignment in the Multilayers of Carboxylic Acids on Silver.
Phys. Rev. Appl., accepted.



13 Vision: Metal-Organic Networks on 2D Materials

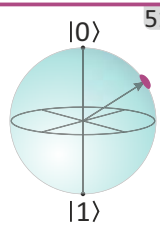
Metal-organic networks self-assembled from metal atoms and small organic molecules present large arrays of equally-spaced magnetic centers in the same local environment (see box 50). The magnetic centers can be employed for magnetic and spintronic applications but also as quantum bits, i.e., the functional units of a quantum computer (see box 51). When multiple spin centers reside in close proximity, indirect magnetic interactions can cause the spins to arrange in specific patterns. The presence of these interactions is generally desirable, but the ideal strength of the interactions depends on the application: it should be dramatically larger in a spin waveguide than in a system intended for quantum computing.^{55,56} This motivates us to search for ways to control the properties of magnetic interactions by external parameters. The charge carrier concentration and polarity within graphene can be externally tuned by an external electric field.

Magnetic coupling of spin centers on surfaces can be mediated by RKKY (Ruderman-Kittel-Kasuya-Yosida) interactions⁵⁷ or by superexchange via the negatively charged ligand⁵⁸. In the case of RKKY, the coupling is mediated by the conduction electrons of the substrate, and exhibits an oscillatory ferromagnetic-antiferromagnetic behavior and a strong dependence on the distance with the charge carrier concentration as one of the defining parameters. In the case of superexchange, the magnetic coupling is reached via the Heisenberg exchange coupling between spins localized at metal sites and the itinerant spin density of the spin-polarized molecular LUMO band. The electronic density of molecular states was shown to be controllable by a gate voltage⁵⁹ applied on the graphene layer giving the promise of control of superexchange interaction strength via adjusting the Fermi level of the graphene layer. Hence, both coupling mechanisms are sensitive to the charge transfer into the substrate and can be, in principle, externally controlled.



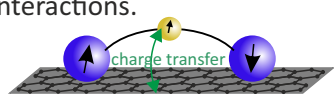
FEATURE 51

Quantum bits (qubits).
Qubits can be placed into a quantum superposition of constituent states, thereby, simultaneously accessing multiple states.




Qubits in metal-organic frameworks.
Qubits can be installed in metal-organic frameworks via a selection of proper structural nodes and linking moieties. Magnetic interactions between qubits are open to synthetic fine-tuning via a proper choice of bridging units.

We propose to use graphene to finely tune the magnetic interactions.



Key reference:
M. J. Graham et al.,
Chem. Mater.
29 (2017), 1885.



Legend:
● = qubit
— = linking group

Obtaining gated graphene devices working in UHV is challenging due to residues from lithographic processing on the graphene substrate. To circumvent the need for lithography, we have developed contactless methods to dope graphene employing X-rays or low-energy electrons (see box 52).^{60,61} The irradiation-induced charge trapped in the dielectric layer acts in the same way as a gate electrode and can provide higher doping than the standard way.

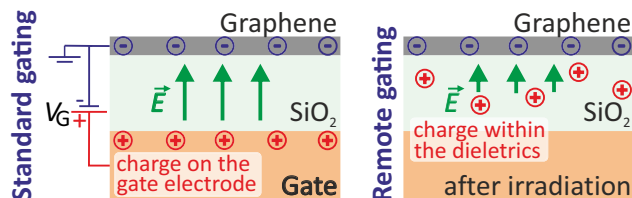
Topological insulators have been attracting attention thanks to their fascinating properties (see box 53)⁶² and possess enormous potential for spintronics and quantum computing applications. Although it is the time-reversal symmetry that topologically protects the electrons from backscattering, an interesting consequence arises upon its breaking, e.g., by the presence of ferromagnetic order (see box 53).⁶³ This potentially leads to the emergence of a quantum anomalous Hall effect.⁶²

We have proposed to prepare a periodic array of magnetic atoms/ions embedded in the 2D metal-organic network (MON).²² The careful design of organic ligands and a proper selection of metal atoms allow fine-tuning of the MON properties, e.g., the type of lattice and its periodicity, molecule-substrate charge transfer, separation of the metal atom from the substrate. It is theoretically predicted that local magnetic moments of 3d atoms are not quenched in a metal-organic network on top of a topological insulator surface, and there is a significant exchange interaction between these atoms.⁶⁴ Hence, the magnetic proximity effect can be achieved by properly designed MONs.

X-RAY AND ELECTRON-BEAM DOPING

52

X-ray exposure of a graphene device causes the formation of electron-hole pairs in the gate dielectrics. The electrons are very mobile and quickly leave the dielectrics. Holes diffuse very slowly and can be eventually captured and immobilized by defects. These defects become charged and electrostatically dope the graphene.



Low energy electrons work similarly, but they can provide both positive and negative doping depending on the gate voltage during the irradiation.

Read full stories here:

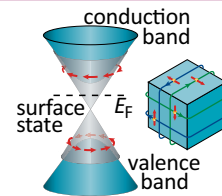


FEATURE

53

Topological insulators (TIs).

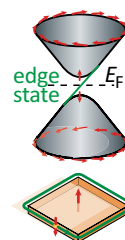
As a consequence of the strong spin-orbit coupling, the bandgap in TIs gets inverted; this gives rise to a special type of surface state.



In these states, the electron's spin is locked to its momentum: they are topologically protected, i.e., robust against surface defects or disorder. This property leads to a nearly dissipation-less current.

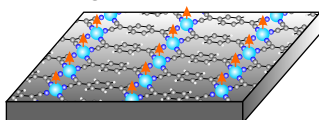
Quantum anomalous Hall effect (QAHE).

Breaking time-reversal symmetry, e.g., by the presence of ferromagnetic (FM) order, leads to the formation of an exchange gap in the band dispersion. Tuning the Fermi level in the exchange gap results in the emergence of a quantum Hall effect at zero magnetic fields, that is, a QAHE. The QAHE is characterized by the formation of dissipation-less 1D chiral edge conduction channels.



This can be realized by periodic arrays of transition metals in metal-organic networks.

Metal-organic network on Bi₂Se₃



Key reference:

Y. Tokura et al.,
Nat. Rev. Phys.
1 (2019), 126.



KEY PUBLICATION

Z. Jakub, et al.: Remarkably Stable Metal-Organic Frameworks on an Inert Substrate: M-TCNQ on Graphene (M = Mn, Fe, Ni). *Nanoscale* **14** (2022), 9507.



14 Research Group: Molecular Nanostructures at Surfaces

The results presented and visions we are working on cannot be carried out by a single person. Without the group working on the realization of our research vision, there would be much less to present. The research group named Molecular Nanostructures at Surfaces was established as a junior research group in January 2018 based on the successful application in an open call. The group was promoted to a “standard” RG in 2020 based on the ISAB evaluation assessing the group’s performance. The brief history of the group is sketched in the timeline below.

The research focus of the group lies in surface-confined supramolecular systems. Our vision is to harness the properties of these systems to provide functionality in electronic and spintronic devices and quantum computing. In this respect, we work on reducing the contact resistance in organic semiconductor devices, as described in Section 12. In a second direction (Section 13) we aim for the realization of externally tunable arrays of magnetic atoms that can be employed in the advanced spintronic/magnonic devices or as a quantum registry. Similar systems on topological insulators may provide material showing the quantum anomalous Hall effect. As the realization of these material systems is not a trivial task, we also aim to understand the principles of self-assembly and the thermodynamics and kinetics of the growth of molecular systems that are close to thermodynamic equilibrium as a necessary first step. The presented research directions can lead to discoveries that globally reduce energy consumption or provide new concepts of advanced devices such as a digital quantum computer.

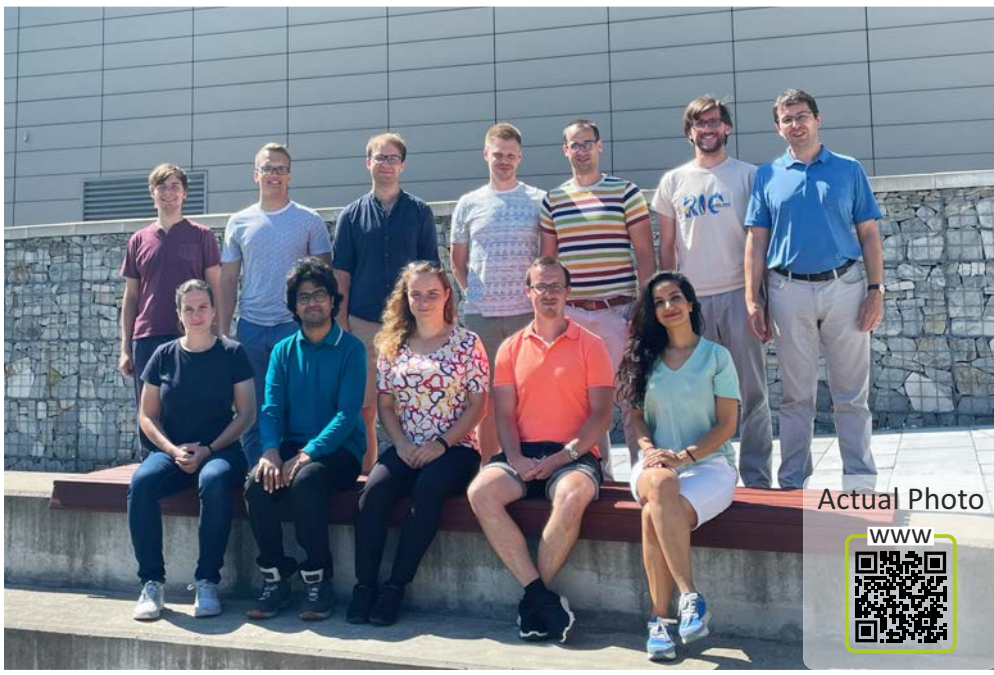
CONVERSATION

You can reproduce all experiments for a publication in a week.


Nice. It is 156 papers in my Ph.D.

It takes two years to realize what to reproduce.

GROUP PHOTO



Actual Photo



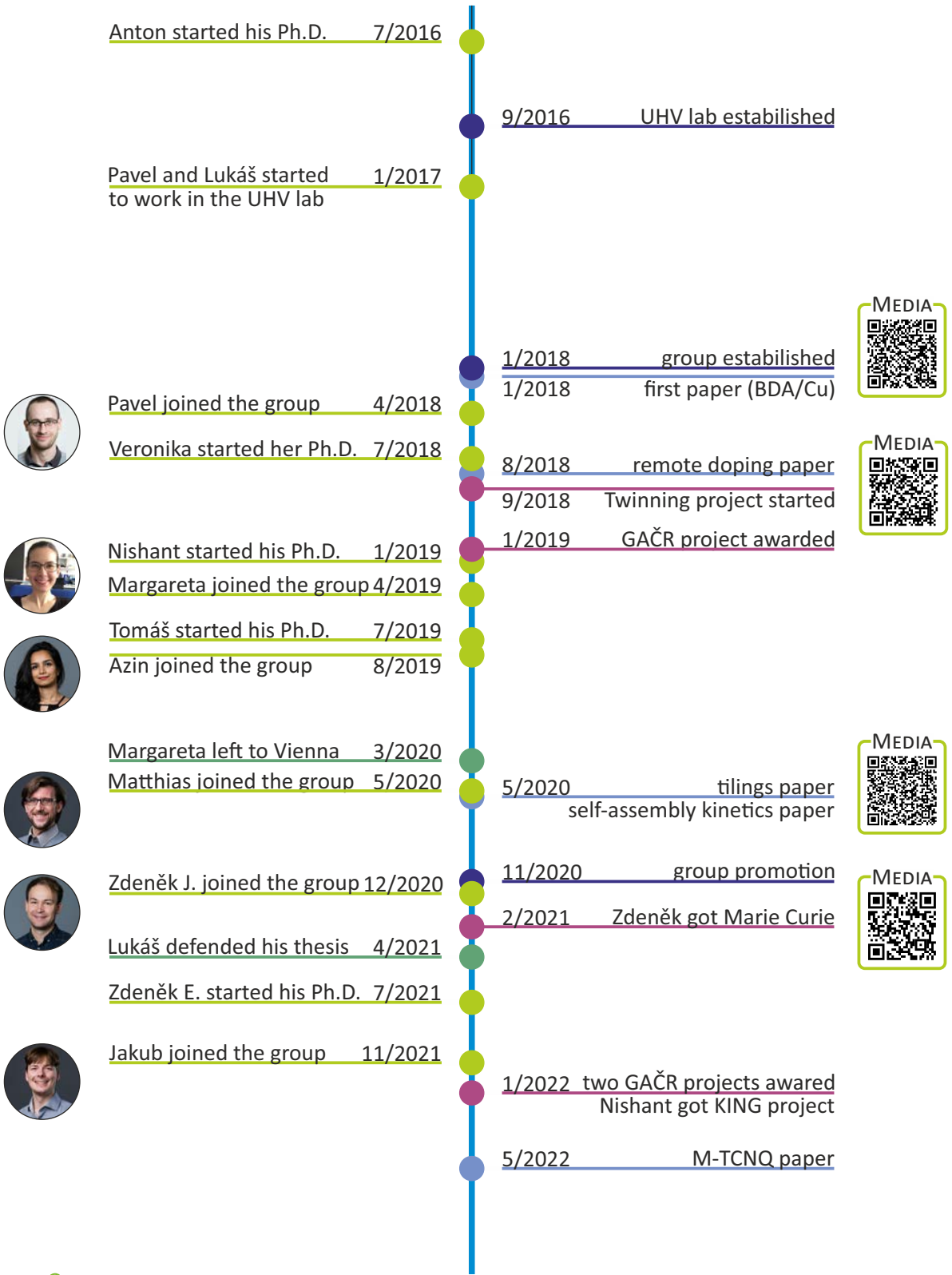
REFERENCES

Group Pages 

Members 

Publications 

Projects 



References

- [1] J. V. Barth, G. Costantini, and K. Kern. Engineering atomic and molecular nanostructures at surfaces. *Nature*, 437:671–679, 2005.
- [2] X.-B. Li, C.-H. Tung, and L.-Z. Wu. Semiconducting quantum dots for artificial photosynthesis. *Nature Reviews Chemistry*, 2:160–173, 2018.
- [3] J. A. Schuller, E. S. Barnard, W. Cai, Y. C. Jun, J. S. White, and M. L. Brongersma. Plasmonics for extreme light concentration and manipulation. *Nature Materials*, 9:193–204, 2010.
- [4] K. S. Novoselov, A. Mishchenko, A. Carvalho, and A. H. Castro Neto. 2D materials and van der Waals heterostructures. *Science*, 353:aac9439, 2016.
- [5] L. Liu and A. Corma. Metal catalysts for heterogeneous catalysis: From single atoms to nanoclusters and nanoparticles. *Chemical Reviews*, 118(10):4981–5079, 2018.
- [6] D. P. Goronzy, M. Ebrahimi, F. Rosei, Arramel, Y. Fang, S. De Feyter, S. L. Tait, C. Wang, P. H. Beton, A. T. S. Wee, P. S. Weiss, and D. F. Perepichka. Supramolecular Assemblies on Surfaces: Nanopatterning, Functionality, and Reactivity. *ACS Nano*, 12:7445–7481, 2018.
- [7] A. Langner, S. L. Tait, N. Lin, C. Rajadurai, M. Ruben, and K. Kern. Self-recognition and self-selection in multicomponent supramolecular coordination networks on surfaces. *Proceedings of the National Academy of Sciences*, 104:17927–17930, 2007.
- [8] L. Grill and S. Hecht. Covalent on-surface polymerization. *Nature Chemistry*, 12:115–130, 2020.
- [9] S. Clair and D. G. de Oteyza. Controlling a Chemical Coupling Reaction on a Surface: Tools and Strategies for On-Surface Synthesis. *Chemical Reviews*, 119:4717–4776, 2019.
- [10] B. Yang, B. Dong, and L. Chi. On-Surface Intramolecular Reactions. *ACS Nano*, 14:6376–6382, 2020.
- [11] L. Grossmann, B. T. King, S. Reichlmaier, N. Hartmann, J. Rosen, W. M. Heckl, J. Björk, and M. Lackinger. On-surface photopolymerization of two-dimensional polymers ordered on the mesoscale. *Nature Chemistry*, 13:730–736, 2021.
- [12] R. M. Tromp. Low-energy electron microscopy. *IBM J. Res. Develop.*, 44:503–516, 2000.
- [13] J. de la Figuera and K. F. McCarty. *Low-Energy Electron Microscopy*, pages 531–561. Springer Berlin Heidelberg, Berlin, Heidelberg, 2013. ISBN 978-3-642-34243-1.
- [14] P. Procházka, M. A. Gosalvez, L. Kormoš, B. de la Torre, A. Gallardo, J. Alberdi-Rodríguez, T. Chutora, A. O. Makoveev, A. Shahsavari, A. Arnau, P. Jelínek, and

-
- J. Čechal. Multiscale Analysis of Phase Transformations in Self-Assembled Layers of 4,4'-Biphenyl Dicarboxylic Acid on the Ag(001) Surface. *ACS Nano*, 14:7269–7279, 2020.
- [15] L. Kormoš, P. Procházka, A. O. Makoveev, and J. Čechal. Complex k-uniform tilings by a simple bitopic precursor self-assembled on Ag(001) surface. *Nature Communications*, 11:1856, 2020.
- [16] P. Procházka, L. Kormoš, A. Shahsavar, V. Stará, A. O. Makoveev, T. Skála, M. Blatnik, and J. Čechal. Phase transformations in a complete monolayer of 4,4'-biphenyldicarboxylic acid on Ag(001). *Applied Surface Science*, 547:149115, 2021.
- [17] K. L. Svane and B. Hammer. Thermodynamic aspects of dehydrogenation reactions on noble metal surfaces. *The Journal of Chemical Physics*, 141:174705, 2014.
- [18] J. Čechal, C. S. Kley, T. Kumagai, F. Schramm, M. Ruben, S. Stepanow, and K. Kern. Convergent and divergent two-dimensional coordination networks formed through substrate-activated or quenched alkynyl ligation. *Chemical Communications*, 50:9973–9976, 2014.
- [19] M. Fritton, D. A. Duncan, P. S. Deimel, A. Rastgoo-Lahrood, F. Allegretti, J. V. Barth, W. M. Heckl, J. Björk, and M. Lackinger. The Role of Kinetics versus Thermodynamics in Surface-Assisted Ullmann Coupling on Gold and Silver Surfaces. *Journal of the American Chemical Society*, 141:4824–4832, 2019.
- [20] S. Bedwani, D. Wegner, M. F. Crommie, and A. Rochefort. Strongly Reshaped Organic-Metal Interfaces: Tetracyanoethylene on Cu(100). *Physical Review Letters*, 101:216105, 2008.
- [21] T.-C. Tseng, C. Urban, Y. Wang, R. Otero, S. L. Tait, M. Alcamí, D. Écija, M. Trelka, J. M. Gallego, N. Lin, M. Konuma, U. Starke, A. Nefedov, A. Langner, C. Wöll, M. Á. Herranz, F. Martín, N. Martín, K. Kern, and R. Miranda. Charge-transfer-induced structural rearrangements at both sides of organic/metal interfaces. *Nature Chemistry*, 2:374–379, 2010.
- [22] C. S. Kley, J. Čechal, T. Kumagai, F. Schramm, M. Ruben, S. Stepanow, and K. Kern. Highly adaptable two-dimensional metal-organic coordination networks on metal surfaces. *Journal of the American Chemical Society*, 134:6072–6075, 2012.
- [23] J. I. Pascual, J. V. Barth, G. Ceballos, G. Trimarchi, A. De Vita, K. Kern, and H. P. Rust. Mesoscopic chiral reshaping of the Ag(110) surface induced by the organic molecule PVBA. *Journal of Chemical Physics*, 120:11367–11370, 2004.
- [24] L. Dong, Z. A. Gao, and N. Lin. Self-assembly of metal–organic coordination structures on surfaces. *Progress in Surface Science*, 91:101–135, 2016.

-
- [25] M. L. Merrick, W. Luo, and K. A. Fichthorn. Substrate-mediated interactions on solid surfaces: Theory, experiment, and consequences for thin-film morphology. *Progress in Surface Science*, 72:117–134, 2003.
- [26] F. Queck, O. Krejčí, P. Scheuerer, F. Bolland, M. Otyepka, P. Jelínek, and J. Repp. Bonding Motifs in Metal-Organic Compounds on Surfaces. *Journal of the American Chemical Society*, 140:12884–12889, 2018.
- [27] T. W. White, N. Martsinovich, A. Troisi, and G. Costantini. Quantifying the “Subtle Interplay” between Intermolecular and Molecule–Substrate Interactions in Molecular Assembly on Surfaces. *The Journal of Physical Chemistry C*, 122:17954–17962, 2018.
- [28] L. Kormoš, P. Procházka, T. Šikola, and J. Čechal. Molecular Passivation of Substrate Step Edges as Origin of Unusual Growth Behavior of 4,4'-Biphenyl Dicarboxylic Acid on Cu(001). *Journal of Physical Chemistry C*, 122:2815–2820, 2018.
- [29] T. Schmitt, L. Hammer, and M. A. Schneider. Evidence for On-Site Carboxylation in the Self-Assembly of 4,4'-Biphenyl Dicarboxylic Acid on Cu(111). *Journal of Physical Chemistry C*, 120:1043–1048, 2016.
- [30] W. D. Xiao, Y. H. Jiang, K. Ait-Mansour, P. Ruffieux, H. J. Gao, and R. Fasel. Chiral biphenyldicarboxylic acid networks stabilized by hydrogen bonding. *Journal of Physical Chemistry C*, 114:6646–6649, 2010.
- [31] Hans Lüth. *Solid Surfaces, Interfaces and Thin Films*. Springer Berlin Heidelberg, 6th edition, 2015.
- [32] Johannes Kepler. *Harmonices Mundi*. Johann Planck, Linz, 1619.
- [33] B. Grünbaum and G. C. Shephard. *Tilings and Patterns: Second Edition*. Dover Publications Inc., 2016.
- [34] M. O. Blunt, J. C. Russell, M. d. C. Gimenez-Lopez, J. P. Garrahan, X. Lin, M. Schroder, N. R. Champness, and P. H. Beton. Random Tiling and Topological Defects in a Two-Dimensional Molecular Network. *Science*, 322:1077–1081, 2008.
- [35] A. Stannard, J. C. Russell, M. O. Blunt, C. Salesiotis, M. D. C. Giménez-López, N. Taleb, M. Schröder, N. R. Champness, J. P. Garrahan, and P. H. Beton. Broken symmetry and the variation of critical properties in the phase behaviour of supramolecular rhombus tilings. *Nature Chemistry*, 4:112–117, 2012.
- [36] S. Whitelam, I. Tambllyn, P. H. Beton, and J. P. Garrahan. Random and Ordered Phases of Off-Lattice Rhombus Tiles. *Physical Review Letters*, 108:035702, 2012.
- [37] U. Schlickum, R. Decker, F. Klappenberger, G. Zoppellaro, S. Klyatskaya, W. Auwärter, S. Neppel, K. Kern, H. Brune, M. Ruben, and J. V. Barth. Chiral kagomé lattice from simple ditopic molecular bricks. *Journal of the American Chemical Society*, 130:11778–11782, 2008.

-
- [38] D. Ecija, J. I. Urgel, A. C. Papageorgiou, S. Joshi, W. Auwärter, A. P. Seitsonen, S. Klyatskaya, M. Ruben, S. Fischer, S. Vijayaraghavan, J. Reichert, and J. V. Barth. Five-vertex Archimedean surface tessellation by lanthanide-directed molecular self-assembly. *Proceedings of the National Academy of Sciences*, 110:6678–6681, 2013.
- [39] Y.-Q. Zhang, M. Paszkiewicz, P. Du, L. Zhang, T. Lin, Z. Chen, S. Klyatskaya, . Ruben, A. P. Seitsonen, J. V. Barth, and F. Klappenberger. Complex supramolecular interfacial tessellation through convergent multi-step reaction of a dissymmetric simple organic precursor. *Nature Chemistry*, 10:296–304, 2018.
- [40] R. Sarkar, K. Guo, C. N. Moorefield, M. J. Saunders, C. Wesdemiotis, and G. R. Newkome. One-Step Multicomponent Self-Assembly of a First-Generation Sierpiński Triangle: From Fractal Design to Chemical Reality. *Angewandte Chemie – International Edition*, 53:12182–12185, 2014.
- [41] S. Coates, J. A. Smerdon, R. McGrath, and H. R. Sharma. A molecular overlayer with the Fibonacci square grid structure. *Nature Communications*, 9:3435, 2018.
- [42] N. A. Wasio, R. C. Quardokus, R. P. Forrest, C. S. Lent, S. A. Corcelli, J. A. Christie, K. W. Henderson, and S. A. Kandel. Self-assembly of hydrogen-bonded two-dimensional quasicrystals. *Nature*, 507:86–89, 2014.
- [43] J. I. Urgel, D. Écija, G. Lyu, R. Zhang, C.-A. Palma, W. Auwärter, N. Lin, and J. V. Barth. Quasicrystallinity expressed in two-dimensional coordination networks. *Nature Chemistry*, 8:657–662, 2016.
- [44] Y. Chen. Nanofabrication by electron beam lithography and its applications: A review. *Microelectronic Engineering*, 135:57–72, 2015.
- [45] M. Huth, F. Porrati, C. Schwalb, M. Winhold, R. Sachser, M. Dukic, J. Adams, and G. Fantner. Focused electron beam induced deposition: A perspective. *Beilstein Journal of Nanotechnology*, 3:597–619, 2012.
- [46] J. M. White. Using photons and electrons to drive surface chemical reactions. *Journal of Molecular Catalysis A: Chemical*, 131:71–90, 1998.
- [47] C. R. Arumainayagam, H. L. Lee, R. B. Nelson, D. R. Haines, and R. P. Gunawardane. Low-energy electron-induced reactions in condensed matter. *Surface Science Reports*, 65: 1–44, 2010.
- [48] M. Waldrip, O. D. Jurchescu, D. J. Gundlach, and E. G. Bittle. Contact Resistance in Organic Field-Effect Transistors: Conquering the Barrier. *Advanced Functional Materials*, 30:1–31, 2020.
- [49] P. Hurdax, M. Hollerer, P. Puschnig, D. Lüftner, L. Egger, M. G. Ramsey, and M. Sterrer. Controlling the Charge Transfer across Thin Dielectric Interlayers. *Advanced Materials Interfaces*, 7:2000592, 2020.

-
- [50] M. P. Das, F. Green, S. M. Bose, S. N. Behera, and B. K. Roul. Dissipation in a Quantum Wire: Fact and Fantasy. In *AIP Conference Proceedings*, volume 1063, pages 26–34. AIP, 2008.
- [51] W. Chen, H. and Zhang, M. Li, G. He, and X. Guo. Interface Engineering in Organic Field-Effect Transistors: Principles, Applications, and Perspectives. *Chemical Reviews*, 120:2879–2949, 2020.
- [52] E. Zojer, T. C. Taucher, and O. T. Hofmann. The Impact of Dipolar Layers on the Electronic Properties of Organic/Inorganic Hybrid Interfaces. *Advanced Materials Interfaces*, 6:1900581, 2019.
- [53] R. Otero, A. L. Vázquez de Parga, and J. M. Gallego. Electronic, structural and chemical effects of charge-transfer at organic/inorganic interfaces. *Surface Science Reports*, 72:105–145, 2017.
- [54] L. Liu, Y. Liu, and X. Duan. Graphene-based vertical thin film transistors. *Science China Information Sciences*, 63:201401, 2020.
- [55] A. Gaita-Ariño, F. Luis, S. Hill, and E. Coronado. Molecular spins for quantum computation. *Nature Chemistry*, 11:301–309, 2019.
- [56] E. Coronado. Molecular magnetism: from chemical design to spin control in molecules, materials and devices. *Nature Reviews Materials*, 5:87–104, 2020.
- [57] N. Abdurakhmanova, T. C. Tseng, A. Langner, C. S. Kley, V. Sessi, S. Stepanow, and K. Kern. Superexchange-mediated ferromagnetic coupling in two-dimensional Ni-TCNQ networks on metal surfaces. *Physical Review Letters*, 110:027202, 2013.
- [58] L. Giovanelli, A. Savoyant, M. Abel, F. Maccherozzi, Y. Ksari, M. Koudia, R. Hayn, F. Choueikani, E. Otero, P. Ohresser, J. M. Themlin, S. S. Dhesi, and S. Clair. Magnetic coupling and single-ion anisotropy in surface-supported Mn-based metal-organic networks. *Journal of Physical Chemistry C*, 118:11738–11744, 2014.
- [59] S. Wickenburg, J. Lu, J. Lischner, H. Z. Tsai, A. A. Omrani, A. Riss, C. Karrasch, A. Bradley, H. S. Jung, R. Khajeh, D. Wong, T. Watanabe, K. and Taniguchi, A. Zettl, A. H. Castro Neto, S. G. Louie, and M. F. Crommie. Tuning charge and correlation effects for a single molecule on a graphene device. *Nature Communications*, 7, 2016.
- [60] P. Procházka, D. Mareček, Z. Lišková, J. Čechal, and T. Šikola. X-ray induced electrostatic graphene doping via defect charging in gate dielectric. *Scientific Reports*, 7:563, 2017.
- [61] V. Stará, P. Procházka, D. Mareček, T. Šikola, and J. Čechal. Ambipolar remote graphene doping by low-energy electron beam irradiation. *Nanoscale*, 10:17520, 2018.

-
- [62] Y. Tokura, K. Yasuda, and A. Tsukazaki. Magnetic topological insulators. *Nature Reviews Physics*, 1:126–143, 2019.
- [63] L. A. Wray, S.-Y. Xu, Y. Xia, D. Hsieh, A. V. Fedorov, Y. S. Hor, R. J. Cava, A. Bansil, H. Lin, and M. Z. Hasan. A topological insulator surface under strong Coulomb, magnetic and disorder perturbations. *Nature Physics*, 7:32–37, 2011.
- [64] M. M. Otrokov, E. V. Chulkov, and A. Arnau. Breaking time-reversal symmetry at the topological insulator surface by metal-organic coordination networks. *Physical Review B*, 92:165309, 2015.

Rights and Permissions

Figures or their parts in the graphical boxes were reproduced with permission from the respective publishers:

Box 5: Reprinted by permission from Springer Nature: T. Kim et al. *Nature* **586** (2020), 385–389, copyright 2020.

Box 9: Adapted from S. Stepanow et al., *J. Phys.: Condens. Matter* **20** (2008), 184002 with permission from the IOP.

Box 10: Reprinted by permission from Springer Nature: ref. 1, copyright 2005.

Box 28: Adapted with permission from F. Wu et al., *Nano Lett.* **22** (2022), 2915–2922. Copyright 2022 American Chemical Society.

Box 32: Adapted from A. Baronov et al., *Phys. Chem. Chem. Phys.* **17** (2015), 20846 with permission from the PCCP Owner Societies.

Box 34: Reproduced from ref. 27 published under CC BY 4.0 licence.

Box 48: Reprinted by permission from Springer Nature: S. Fratini et al., *Nat. Mater.* **19** (2020), 491–502, copyright 2020.

Box 49: Reprinted by permission from Springer Nature: ref. 54, copyright 2020.

Box 51: Reproduced from ref. 65 published under CC BY 4.0 licence.

Box 53: Reprinted by permission from Springer Nature: ref. 62 , copyright 2019.

Abstract

This thesis introduces the field of molecular self-assembly on solid surfaces in the broader perspective of the field of nanotechnology and presents my contribution to the field. In the introductory part, we outline the main conceptual aims of nanotechnology, molecular self-assembly, and fundamentals of employed experimental techniques. The second part describes our main results: the temperature-induced chemical transformation of our model molecule, biphenyl-4,4'-dicarboxylic acid, on silver substrates, emphasizing the transformation kinetics, geometrical representations of observed molecular phases, and electronic properties of the interface. Finally, we present our long-term visions: creating efficient electrode-organic semiconductor interfaces, externally tunable arrays of magnetic moments, and material systems displaying the quantum anomalous Hall effect.

Abstrakt

Tato práce představuje obor molekulárního samouspořádávání na površích pevných látek v širším kontextu oblasti nanotechnologií a prezentuje vlastní přínos k tomuto oboru. V úvodní části nastiňujeme principiální cíle nanotechnologie, molekulárního samouspořádávání a základy použitých experimentálních technik. V druhé části popisujeme naše stěžejní výsledky: teplotně indukovanou chemickou transformaci kyseliny biphenyl-4,4'-dicarboxylové na površích stříbra, přičemž klademe důraz na kinetiku transformace, geometrickou reprezentaci molekulárních fází a elektronické vlastnosti rozhraní. Nakonec představujeme naše dlouhodobé vize: vytvoření efektivních rozhraní mezi elektrodou a organickým polovodičem, externě říditelných polí magnetických momentů a realizaci systému vykazujícího kvantový anomální Hallův jev.